Syst. Biol. 0(0):1–21, 2026

https://doi.org/10.1093/sysbio/syag035
Advance Access publication April 20, 2026

Phylogenomic Discordances Reveal Conflicting Hybridization Episodes and Widespread Lineage-Sorting Events in Temperate Loliinae Grasses

María Fernanda Moreno-Aguilar[1,*,†], Chunlin Chen[1,†], Juan Viruel[1,2], Diana Calderón[1], Itziar Arnelas[3,4], Aminael Sánchez-Rodríguez[4], Wenli Chen[5], Juan Camilo Ospina[6], Gloria Martínez-Sagarra[7], Juan Antonio Devesa[7], Alan Stewart[8], and Pilar Catalán[1,9,*]

[1]*Departamento de Ciencias Agrarias y del Medio Natural, Escuela Politécnica Superior de Huesca, Universidad de Zaragoza, C/ Ctra. Cuarte Km 1, E-22071 Huesca, Spain*
[2]*Royal Botanic Gardens, Kew, Richmond, Surrey, TW9 3AE, United Kingdom*
[3]*Departamento de Biodiversidad, Ecología y Evolución, Facultad de Ciencias Biológicas, Universidad Complutense de Madrid, 28040 Madrid, Spain*
[4]*Departamento de Ciencias Biológicas y Agropecuarias, Universidad Técnica Particular de Loja, San Cayetano Alto s/n, CP 11-01-608 Loja, Ecuador*
[5]*State Key Laboratory of Plant Diversity and Specialty Crops, Institute of Botany, Chinese Academy of Sciences, Beijing 100093, China*
[6]*Facultad de Ciencias Agrarias, Universidad Nacional de Jujuy, Av. Bolivia 1239, San Salvador de Jujuy, Y4600 Jujuy, Argentina*
[7]*Departamento de Botánica, Ecología y Fisiología Vegetal, Universidad de Córdoba, Campus de Rabanales, E-14014 Córdoba, Spain*
[8]*PGG Wrightson Seeds Ltd., PO Box 69 132, Lincoln, Christchurch 7640, New Zealand*
[9]*Grupo de Bioquímica, Biofísica y Biología Computacional (BIFI, UNIZAR), Unidad Asociada al CSIC, E-50059 Zaragoza, Spain*
[*]*Correspondence to be sent to: Pilar Catalán, Departamento de Ciencias Agrarias y del Medio Natural, Escuela Politécnica Superior de Huesca, Universidad de Zaragoza, C/ Carretera de Cuarte Km 1, E-22071 Huesca, Spain; E-mail: pcatalan@unizar.es. María Fernanda Moreno Aguilar, Departamento de Ciencias Agrarias y del Medio Natural, Escuela Politécnica Superior de Huesca, Universidad de Zaragoza, C/ Carretera de Cuarte Km 1, E-22071 Huesca, Spain; E-mail: 770284@unizar.es.*
[†]*Both authors contributed equally as first coauthors.*

Received 22 August 2025; reviews returned 6 April 2026; accepted 8 April 2026
Associate Editor: Tiina Särkinen

Abstract.—The grass subtribe Loliinae has great ecological and economic importance, as it includes community-dominant species of mountain grasslands and the most extensively cultivated pasture, fodder, and turf grasses (fescues, ryegrasses). Resolving the phylogeny of recently evolved Loliinae lineages has proven challenging due to frequent introgressions and polyploidizations that occurred throughout their history. Here, we present the first target capture phylogeny of Loliinae using 270 orthologous single-copy nuclear coding loci for a large sample of 132 representative taxa, covering all its 29 evolutionary lineages. Additionally, we assembled plastome sequences to complement the inferred hybrid speciation history of the Loliinae. Concatenated maximum likelihood and multispecies coalescent trees of ortho-homeolog single-copy genes showed well-supported relationships for major lineages, which were generally consistent across analyses and genomes, and with previous taxonomic and phylogenetic findings. However, they also revealed high levels of both nuclear and cytonuclear discordances estimated to be caused by hybridization and incomplete lineage sorting. We complemented this with a phylogenetic network analysis with representative samples from the main clades to infer reticulation events in the evolution of these grasses. Furthermore, we performed gene tree–species tree reconciliation methods using gene duplication and loss models and multi-labeled trees for polyploidy analysis to estimate the proportion of duplicated genes and the nature of polyploidy of the major Loliinae lineages. These analyses agreed that the fine-leaved (FL) Loliinae clade could have evolved from hybridization between more ancestral broad-leaved (BL) Loliinae lineages and that both groups underwent ancestral and recent hybridizations. The time-calibrated phylogeny of for the main Loliinae clades supports an early Miocene origin for Loliinae and Mid-Late Miocene splits for its main BL and FL lineages, whereas current species-rich groups radiated in the Late Miocene. Hybridization tests of nuclear data and topological incongruence assays between the nuclear single-copy genes and plastome-based trees using various approaches and different sampling subsets confirmed the rampant hybridization experienced by Loliinae at deep and shallow nodes. However, hybridization rates differed from lineage to lineage within the major clades and were not correlated with time or ploidy level, but rather depended on their different propensities to hybridize with species within and/or outside their own clade. Our analyses detected high hybridization rates in four BL (Subulatae-Hawaiian, Tropical-South African, Mexico-Central-South American [MCSA I–II], and Leucopoa p.p.) and five FL Loliinae lineages (American II, Aulaxyper, Afroalpine, American-Neozeylandic, and Australia-Tasmania) containing rogue species that probably originated from trans-clade crosses and are more likely to hybridize greatly. In contrast, they recovered low hybridization rates in four BL (Schedonorus-Lolium, Subbulbosae, Drymanthele-Pseudoscariosae-Lojaconoa, and Leucopoa p.p.) and six fine-leaved lineages (Festuca, Psilurus-Vulpia, American I, Exaratae-Loretia, American-Vulpia-Pampas, and Eskia), with species derived from single ancestors that hybridize only with close congeners. Inferences from gene duplications and allopolyploidizations, along with inheritance probabilities from the phylogenetic network, point to the BL Loliinae lineages as ancient hybrids or paleo-allopolyploids, whereas the FL lineages, especially those of the core FL clade, correspond to more recent meso- or neo-allopolyploids. [Allopolyploidization; *Festuca* and related genera; lineage-specific hybridization rates; nuclear and cytonuclear discordances; nuclear single-copy genes; phylogenomics; plastome.]

Reconstructing the phylogenetic relationships of large groups of organisms is often challenging because their evolutionary histories are shaped by processes that violate simple bifurcating models. Hybridization, polyploidization, genome fractions gains and losses, and lateral gene transfers can obscure phylogenetic signal and generate conflicting topologies across loci (Marcussen et al. 2015; Dunning et al. 2019; Liu et al. 2019; Cui et al. 2025). These difficulties are particularly pronounced in plant lineages with extensive reticulate evolution, where repeated introgression events and auto- or allopolyploidization followed by diploidizations have occurred frequently and independently across lineages (Soltis et al. 2016; Mandáková and Lysak 2018; Sancho et al. 2022).

Phylogenetic networks provide a framework to model such reticulate histories by incorporating hybridization and/or polyploidization events into evolutionary reconstructions (Huber et al. 2006). However, accurate inference of these networks depends on the availability of gene trees that adequately represent all parental subgenomes, which is often difficult in allopolyploid complexes (Marcussen et al. 2015). Coalescent-based approaches applied to multilocus and multigenomic data sets offer an alternative by explicitly accounting for incomplete lineage sorting (ILS), introgression, and gene duplication, thereby improving phylogenetic inference across different taxonomic scales (Baker et al. 2022). In this context, target capture of hundreds of nuclear genes has become a powerful tool for phylogenomic studies, particularly in non-model plant groups and in taxa represented mainly by historical collections (Johnson et al. 2019; Pérez-Escobar et al. 2021; Thomas et al. 2021; Zuntini et al. 2021; Baker et al. 2022). Recent methodological advances that quantify gene tree conflict and cytonuclear discordance further enable the dissection of complex evolutionary histories and the testing of hypothesis linking reticulation to morphological diversification (Pérez-Escobar et al. 2016; Minh et al. 2020; Hendriks et al. 2023).

The grass subtribe Loliinae represents one of the most diverse lineages within cool seasonal pooid grasses (Catalán 2006). It includes more than 600 species, many of which have major ecological and economic importance as dominant components of grassland ecosystems and as widely cultivated pasture, forage, and turf grasses, such as fescues and ryegrasses. Loliinae species occur mainly in temperate regions and tropical mountain systems across all continents except Antarctica (Minaya et al. 2017; Moreno-Aguilar et al. 2020; Moreno-Aguilar, 2022a). The group comprises the large genus *Festuca*, with more than 500 species, together with 13 smaller but closely related genera that together include about 50 species (Catalán 2006; Catalán et al. 2004; Catalán et al. 2007; Moreno-Aguilar, 2022a). *Festuca* and four genera (*Megalachne*, *Micropyropsis*, *Podophorus*, and *Pseudobromus*) contain perennial species, and the remaining nine consist exclusively (*Ctenopsis*, *Dielsiochloa*, *Hellerochloa*, *Micropyrum*, *Narduroides*, *Psilurus*, *Vulpia*, and *Wangenheimia*) or predominantly (*Lolium*) of annual species.

Despite their morphological diversity, Loliinae species share a conserved chromosome base number of $x = 7$ and exhibit a wide range of ploidy levels, from diploid ($2n = 2x = 14$) to high-level polyploid ($2n = 14x = 98$) (Martínez-Sagarra et al. 2021). Hybridization and polyploidization are pervasive, particularly within *Festuca*, where most species are allopolyploid and southern hemisphere taxa are exclusively polyploids (Dubcovsky and Martínez 1992; Catalán 2006; Šmarda et al. 2008; Moreno-Aguilar, 2022a). Biogeographic reconstructions based on dispersal-extinction-cladogenesis (DEC) models suggest that the two major lineages of Loliinae, broad-leaved (BL) and fine-leaved (FL), originated in the northern hemisphere and later colonized the southern continents, where polyploid lineages diversified extensively (Minaya et al. 2017).

Previous phylogenetic and taxonomic studies have provided a foundational framework for understanding the evolution of Loliinae. Within this subtribe, *Festuca* has been shown to be paraphyletic, and its species have been classified into 12 subgenera following Alexeev's worldwide taxonomic treatment, with further subdivision into sections and subsections by different authors, whereas several species remain unranked at the supraspecific level (Supplementary Table S1; Catalán et al. 2007; Moreno-Aguilar, 2022a, and references therein). Early phylogenetic analyses based on a limited number of nuclear markers (ITS, *b-amylase*, *GBSS*) and plastid loci (*trn*TL, *trn*LF) provided a preliminary evolutionary framework for Loliinae (Inda et al. 2008; Díaz-Pérez et al. 2014; Minaya et al. 2015, Minaya et al. 2017). These studies consistently demonstrated that Loliinae is divided into two major evolutionary lineages, BL and FL, each comprising several subordinate lineages that were recovered across both nuclear and plastid-based topologies.

More recent phylogenetic work using genome skimming approaches reconstructed Loliinae relationships from complete plastome sequences and nuclear 35S and 5S rDNA loci (Moreno-Aguilar et al. 2020; Moreno-Aguilar, 2022a). These analyses were broadly congruent with earlier multilocus phylogenies but revealed increased topological incongruence within particular subclades and expanded the sampling and recognition of additional evolutionary lineages within the subtribe. Successive phylogenies of Loliinae have shown that the BL clade is formed by lineages of nine subgenera of BL *Festuca* (*F.* subgen. *Asperifolia*, *Coironhuecu*, *Drymanthele*, *Erosiflorae*, *Leucopoa*, *Schedonorus*, *Subulatae*, *Subuliflorae*, and *Xanthochloa*) plus three annual or perennial genera (*Lolium* L., *Micropyropsis* Romero Zarco & Cabezudo, and *Pseudobromus* K. Schum.), whereas the FL clade is formed by lineages of FL *F.* subgen. *Festuca* and some BL fescues (*F.* subgen. *Mallopetalon*, *Drymanthele* pro parte) plus 10 annual genera (*Ctenopsis* De Not., *Diel-*

siochloa Pilg., *Hellerochloa* Rauschert, *Megalachne* Steud., *Micropyrum* (Gaudin) Link, *Narduroides* Rouy, *Podophorus* Phil., *Psilurus* Trin., *Vulpia* C.C. Gmel., and *Wangenheimia* Moench) (Catalán 2006; Catalán et al. 2007; Inda et al. 2008; Díaz-Pérez et al. 2014; Minaya et al. 2017; Moreno-Aguilar et al. 2020; Moreno-Aguilar, 2022a).

Complementary analyses of the Loliinae repeatome recovered a consensus network topology that closely matched the nuclear 35S rDNA tree, supporting a scenario of recurrent allopolyploidization followed by partial diploidization. This evolutionary process likely generated the large genome sizes observed in BL diploids, which are significantly larger than those of FL diploids (Moreno-Aguilar et al. 2022b). Despite these advances, phylogenomic inferences for Loliinae based on extensive sampling of single-copy nuclear genes, and their potential congruence with plastome, nuclear ribosomal, and repetitive elements data sets, have not yet been comprehensively assessed.

Here, we present the first large-scale phylogenomic analysis of Loliinae based on target capture data generated with the Angiosperms353 nuclear probe set (Johnson et al. 2019) for 132 taxa representing all currently recognized evolutionary lineages. By integrating these data with whole plastome sequences, we investigate the extent to which hybridization and ILS have shaped the evolutionary history of the group. Specifically, we test whether introgression rates differ between BL and FL Loliinae, whether hybridization is associated with particular lineages, and whether these patterns are related to divergence time or ploidy level. This integrative approach allows us to evaluate lineage-specific reticulation processes and to clarify the complex phylogenetic history of one of the most economically and ecologically important grass groups.

Materials and Methods

Sampling

Samples of 132 species from eight genera of Loliinae (*Festuca*, 118; *Lolium*, 5; *Vulpia*, 4; *Micropyropsis*, 1; *Megalachne*, 1; *Wangenheimia*, 1; *Psilurus*, 1; and *Hellerochloa* , *1*) and three related outgroup grasses (*Oryza sativa*, *Hordeum vulgare*, and *Alopecurus aequalis*) were included in the study (Supplementary Table S1 and Supplementary Fig. S1). The 132 Loliinae samples were first analyzed to capture single-copy nuclear gene targets, 79 of them were analyzed for plastome data for the first time, and 30 were not previously included in phylogenetic studies (Supplementary Table S1). Sampling was carried out from fresh materials collected in the field, collections of silica-dried leaves, and herbarium vouchers (Supplementary Table S1). Plastome data retrieved from 49 previously studied taxa (Moreno-Aguilar, 2022a; Moreno-Aguilar, 2022b) were incorporated into the analysis (Supplementary Table S1). The selected taxa represent the 28 evolutionary lineages currently recognized within Loliinae (Minaya et al. 2017; Moreno-Aguilar, 2022a).

Target Gene Capture and Genome Skimming Sequencing

Genomic library preparation and targeted enrichment of Loliinae single-copy nuclear genes were performed with the Angiosperms353 target capture kit at Arbor Biosciences (Michigan, USA), following the protocols outlined in Johnson et al. (2019). Targeted sequence capture was performed in pools of 12 libraries following the myBaits v5 manual (https://arborbiosci.com/mybaits-manual/). Capture reactions were pooled in equimolar ratios to form a sequencing pool, which was sequenced on a partial lane of the Illumina NovaSeq 6000 platform in paired-end (PE) mode (2 × 150 bp). Output reads from target enrichment sequencing were checked with FastQC (https://www.bioinformatics.babraham.ac.uk/projects/fastqc/) and trimmed (Bolger et al. 2014) preserving reads with a minimum length of 50 bp (minlen: 50) to reduce the risk of potential misalignments of short reads to genes and trimming bases at the end of the reads with low quality (trailing: 30).

Genome skimming sequencing was performed on 79 Loliinae DNA samples at the Centro Nacional de Análisis Genómico (CNAG) and Macrogen (Spain) to assemble their plastome sequence (Supplementary Table S1). Genomic sequencing of a multiplexed pool of PCR-free KAPA libraries was performed on a HiSeq4000 or HiSeq 2500 (TruSeq SBS Kit v4, Illumina, Inc) in PE mode (2 × 101 bp) as described in Moreno-Aguilar et al. (2020). Illumina PE reads were quality-checked using FastQC and adapters and low-quality sequences were trimmed and removed with Trimmomatic. Loliinae genomic samples used in subsequent analysis contained between 1.5 and 35.0 million reads (average 16.0 million reads) with insert sizes ranging between 69 and 260 bp (Supplementary Table S1).

Sequence Assemblies of Target Capture Data, Gene Orthology Assessments, and Hybrid Class Detection (AD and LH metrics)

Loliinae single-copy nuclear genes were recovered from the target-enriched PE reads using the HybPiper v.2.3.2 pipeline (Johnson et al. 2016). This was done by mapping the filtered reads against the template sequences of the 353 low-copy nuclear genes (available at https://github.com/mossmatters/Angiosperms353) using the Burrows-Wheeler Alignment (BWA v.0.7) (Li et al. 2009), and then through de novo assembly of mapped reads for each gene separately using SPAdes v. 3.13 (Bankevich et al. 2012), with the default minimum coverage threshold of 8× (Supplementary Fig. S2). The HybPiper script *paralog_retriever* was used to obtain a data set from Loliinae, made of nuclear single-copy

genes. Following this initial HybPiper assembly step, a total of 352 genes were recovered across the 132 Loliinae samples studied. This unfiltered data set (scg-raw data set; Supplementary Appendix 1), which contains all genetic and allelic diversity, was used for gene duplication analyses and to assess the nature of polyploidy in Loliinae lineages. The homology of these 352 nuclear genes was circumscribed using Orthofinder v. 3.0.1 (Emms and Kelly 2015) to incorporate the coding sequence from the reference genomes of the diploid outgroups *Oryza sativa* (NCBI accession GCF_034140825.1), *Hordeum vulgare* (subsp. *vulgare*) (GCA_904849725.1), and *Alopecurus aequalis* (GCA_964340505.1), and the diploid ingroup *Lolium perenne* (P226/135/16) into the Loliinae gene capture data set. This initial filtering of homologous genes was necessary to select appropriate outgroup reference sequences for the target genes studied in the Loliinae data set and did not affect subsequent tree-based orthology filtering approaches, which focused primarily on ingroup sequences. We then used ASTRAL-Pro (Zhang et al. 2020) to construct a species tree using 325 of the 352 total loci that meet the constraint of fewer than 27 (20% of total taxa) missing taxa. We filtered the 352 groups based on this criterion and the constraint of the maximum number of copies of the same taxon fewer than 5, resulting in a total of 302 homologous clusters. These clusters (scg-full data set; Supplementary Appendix 2) were used for gene tree–species tree reconciliation analysis using Notung and GRAMPA (see below). They were further analyzed using the Yang and Smith (2014) pipeline to obtain orthologs for all Loliinae samples under study. We initially tested all three alternative tree-based orthology inference approaches, including maximum inclusion (MI), monophyletic outgroups (MO), and one-to-one (1-to-1) methods (Yang and Smith 2014). For all these analyses, the minimum number of taxa was 108 (allowing a maximum of 27 missing taxa) and for the MI method the long tip cutoff was set at "0.2." We selected the 270 genes filtered by MI as a strict data set of reliable orthologous single-copy genes (Supplementary Table S2). This was because the 270 gene trees retrieved from MI (scg-strict and inclusive data sets; Supplementary Appendix 3) yielded a consensus phylogeny regarding the placement of major clades (concatenated IQ-TREE2 and ASTRAL trees) similar to those obtained from the 184 gene trees retrieved from MO and the 175 genes retrieved from 1-to-1 (see Results and Supplementary Appendices 3 and 4), but with the highest average bootstrap support (BS) percentages or posterior probability among the three data sets. Furthermore, because the MO process retrieves MO genes and 1-to-1 genes simultaneously, and of the 184 genes retrieved by the MO process, 175 overlap with the 1-to-1 process, we will only show the result of the MO analysis in the supplementary files (see below).

For the HybPiper 270 MI-filtered orthologous single-copy-genes data set (Supplementary Table S2), individual genes were aligned with MAFFT v.7.490 (Katoh and Standley 2013) using the iterative refinement method *–maxiterate* 1000. Empty genes for any Loliinae sample were removed from downstream analysis. trimAl v. 1.2rev59 (Capella-Gutiérrez et al. 2009) was used to remove sequences with insufficient coverage (*-automated1*) in well-occupied columns of each gene alignment. Gene alignments were visually inspected with Geneious Prime to detect potentially misaligned sequences. Sequences with more than 60% of the total alignment length consisting of gaps were removed to enhance the quality of the data sets, filtering out species with potentially low phylogenetic information. This process generated the respective multiple sequence alignments (MSAs). To check alignment quality, we estimated summary statistics of gene alignments using AMAS v.0.98 (Borowiec 2016). These statistics included alignment length, missing data and number of parsimony informative sites.

We used HybPhaser v2.0 (Nauheimer et al. 2021) to detect potential hybrids in our 270 orthogroups data set of Loliinae. This tool maps raw sequence data to the HybPiper contigs taking into account SNP variation using nucleotide ambiguities and quantifying divergence between gene variants. The gene variants correspond either to paralogs or to hybrids ("homeologs" in allopolyploids; Sancho et al. 2022) (Supplementary Table S3). Samples showing high SNP content in genes are likely hybrids or polyploids and are phased for the different copy variants (alleles) into phased haplotypes (Nauheimer et al. 2021; Hendriks et al. 2023). We ran HybPhaser to detect potential hybrid/polyploid samples without ruling out putative "paralogs" and generated a data set of phased accessions of Loliinae (scg-inclusive data set) (Supplementary Table S3 and Supplementary Appendix 3). We used R scripts to compute two metrics indicative of hybridization, sample allele divergence (AD, percentage of SNPs in all genes) and locus heterozygosity (LH, percentage of genes with SNPs). We classified the Loliinae samples into three LH-versus-AD hybrid-type classes [1) low hybrid level: low-to-medium LH ($\geq$10–$\leq$82.4) and low AD ($>$0–$\leq$1.7); 2) medium hybrid level: medium LH ($\geq$70–$<$ 90) and medium AD ($>$1.71–$\leq$2.8); and 3) high hybrid level: high LH ($\geq$80) and high AD ($>$2.8)], which are biologically meaningful and reflect their hybridization history (Nauheimer et al. 2021; Hendriks et al. 2023).

Sequence Assemblies of Plastomes

Whole plastome sequences for 79 new Loliinae samples were assembled from their respective genome skimming PE reads, following the procedures indicated in Moreno-Aguilar et al. (2020). Plastome assembly was performed with Novoplasty v.2.7.1 (Dierckxsens et al. 2017) using the plastome of *Festuca pratensis* (JX871941) as reference sequence and standardized parameters (k-mer: 30–39, insert size: ~69–200 bp, genome range: 120,000–140,000 bp, and PE reads: 101–150 bp). Fur-

thermore, to recover plastome sequences in data with a low number and quality of total PE reads, plastome assembly was performed using a read-mapping strategy to, respectively, closely related *Festuca* plastomes using Geneious Prime (Supplementary Table S1). The data for 49 representative Loliinae taxa from previous studies (Moreno-Aguilar et al. 2020; Moreno-Aguilar, 2022a, Moreno-Aguilar, 2022b) were incorporated into existing plastome data set (Supplementary Table S1 and Supplementary Appendix 5). Whole plastome sequences were aligned separately with MAFFT v.7.031b, and trimAl v. 1.2rev59 was used to remove poor-quality regions from the MSA with the *-automated*1 parameter.

Phylogenomic Reconstructions and Intragenomic Nuclear Discordance

We used three different approaches to analyze our genomic data sets and reconstruct Loliinae phylogenies. First, trimmed MSAs from the Loliinae scg-strict data set (270 MI-filtered genes; Supplementary Table S2 and Supplementary Appendix 3) and different numbers of MO-(184) filtered genes (Supplementary Appendix 4) were concatenated into their respective supermatrices. Subsequently, they were used for maximum likelihood (ML) phylogenetic reconstruction using IQ-TREE2 v. 2.2.2.6 (Nguyen et al. 2015; Minh et al. 2020), applying the "proportional to edges" partitioning model with individual loci as partitions and model selection implemented using ModelFinder (Kalyaanamoorthy et al. 2017) for each partition. Branch support was calculated from 1000 UltraFast Bootstrap replicates (Hoang et al. 2018) and gene concordance factors (gCF) and site concordance factors (sCF, parameter –scf 1000; Minh et al. 2020) for all nodes. Second, individual ML trees of each single-copy nuclear gene, as well as ML trees of the entire plastome MSA, were calculated separately using the same IQ-TREE2 procedure. *Oryza sativa*, *Hordeum vulgare*, and *Alopecurus aequalis* were used to root all trees. Third, to consider potential ILS events between closely related Loliinae lineages, a species tree was inferred by analyzing the Loliinae 270 scg-strict data set under the multispecies coalescence (MSC) using ASTER package v.1–3.5 ASTRAL (Zhang et al. 2025), which was fed with the individual ML gene trees from IQ-TREE2. All gene trees were rooted using *Oryza sativa*, *Hordeum vulgare*, and *Alopecurus aequalis*, with the *pxrr* function in Phyx (Brown et al. 2017), except for four trees that were rooted using the early divergent lineages of *Festuca lasto* and *F. drymeja* as the outgroup. Branches with BS values $< 30\%$ in the gene trees were collapsed using *nw_ed* from Newick Utilities 1.6.0 (Junier and Zdobnov 2010). To estimate intragenomic discordance in the nuclear data set, we analyzed in R the normalized quartet scores generated for the main topology and the first and second alternative topologies when inferring the MSC species tree. An ASTRAL topology was also generated for the MO-(184) data set. Although the MSC model is only consistent when ILS is the sole source of gene tree discordance, comparison with the supermatrix ML tree can identify highly supported clades (Nauheimer et al. 2021).

To further characterize the impact of ILS versus introgression/hybridization (IH) in Loliinae lineages, we estimated the ILS and IH indices using Phytop v.1.0 (Shang et al. 2025), a pipeline that quantitatively assesses ILS/IH magnitudes based on the nodal quartets' supports (q1, q2, q3) derived from an ASTRAL nuclear species tree inferred from 270-MI individual ML gene trees. The inferred species tree served as the reference topology for Phytop comparative analysis, allowing for the quantification and visualization of Loliinae lineage-specific ILS/IH values using topology matching algorithms (Chen et al. 2025; Shang et al. 2025).

Species Network Analysis, Whole-Genome Duplications, and Polyploidy Events

To assess the impact of reticulated evolution on the observed conflicting nodes of the Loliinae nuclear coalescent tree, we applied a phylogenetic network approach based on a maximum pseudo-likelihood method (Yu and Nakhleh 2015) implemented in PhyloNet v. 3.8.0 (Than et al. 2008; Wen et al. 2018) using the 270 scg-strict data set. This approach considers ILS in the coalescent model and hybridization at the reticulating nodes of the network (Keuler et al. 2020). Due to the computational burden, we restricted our searches to 20 species representative of major Loliinae lineages recovered in the IQ-TREE2 and ASTRAL trees (BL: Leucopoa, Tropical-South African, Mexico-Central-South American [MCSA] I, MCSA II, Schedonorus-Lolium; FL: Eskia, American-Neozeylandic, American I, American II, Subulatae-Hawaiian, Afroalpine, Exaratae-Loretia, Aulaxyper, Festuca) and *Oryza sativa* as outgroup. We performed network searches based on the reduced 270 scg-strict gene trees. Missing taxa were also allowed for some orthologous gene trees in this 20-taxa data set. Network searches were performed with the allowed networks (1 for the first search, 2 for the second, and subsequently up to 10 for the tenth). For each search, 10 runs were performed with the parameter "-x 10." The best-fitting networks obtained for each allowed reticulation model were further optimized for branch lengths and inheritance probabilities using a likelihood framework, and the best-fitting network was selected using the bias-corrected Akaike information criterion (AICc, Sugiura 1978) and the Bayesian information criterion (BIC, Schwarz 1978) by applying the number of parameters as the number of branches plus the number of inheritance probabilities [$(2n - 3) + (2h)$, where h is the number of hybridizations in the network], following Morales-Briones et al. (2021). Complementarily, we applied a gene tree reconciliation method to detect gene duplication events in the ASTRAL phylogeny of Loliinae, applying the gene duplication and

loss model implemented in Notung v. 2.6 (Stolzer et al. 2012). The 302 individual ML gene trees (scg-full data set; Supplementary Appendix 2) were used as input with a duplication cost of 1.5, following Koenen et al. (2021). To account for gene tree estimation error, we also filtered out genes whose outgroup did not form a monophyletic clade and whose average bootstrap was less than 60, and rerun Notung with these remaining 167 trees with the same parameters. The 167 filtered individual ML genetic trees were used as input for Notung, following the same procedure for those 302 individual gene trees. The proportion of duplicated genes for each branch was tallied from 302 homologous gene trees and 167 homologous gene trees, respectively. In addition, we assessed whether branches with more than 10% duplicated genes could have undergone allopolyploidization, autopolyploidization, or no-polyploidization, and the identification of the possible parental lineages that formed the allopolyploids, using the species tree reconciliation approach from gene trees to multi-labeled trees with GRAMPA v. 1.4.0 (Thomas et al. 2017). GRAMPA performed least common ancestor reconciliation of all gene family trees against both the singly labeled species tree and all possible multi-labeled (MUL). The program assigned a reconciliation score for each MUL considered and the origin of homologs, scoring polyploid lineages (H1 nodes) together with the possible locations of the second parental lineage (H2 node) to infer genetic origin (Yang et al. 2023). We tested possible Whole Genome Duplication (WGD) scenarios with the lowest parsimony scores by comparing the scores obtained for the singly labelled species tree (not WGD) with those of the MUL tree (the node subject to WGD forms sister branches with descendant paralogs [autopolyploidization] or not [allopolyploidization]) to decide whether WGD was supported by GRAMPA and what type of polyploidization was inferred. In our case, we tested the potential polyploid nodes identified by Notung with more than 10% of gene duplications with all the nodes along the phylogeny and to incorporate more gene copy variation, we used the parameter "-c 14" when running GRAMPA.

Evaluation of Cytonuclear Topological Discordance and Dating Analysis

To assess the degree to which the phylogeny retrieved by the nuclear coding genome agrees with that of the organelle (plastome) genome, we also applied the Procrustean Approach to Cophylogeny (PACo) procedure implemented in R (Balbuena et al. 2013; Hutchinson et al. 2017) to the nuclear 270 scg-strict supermatrix ML trees versus the plastome supermatrix ML trees (bootstrap trees) of 128 common Loliinae species. PACo is a global-fit method used to detect coevolutionary associations between different organisms or different nuclear and (endosymbiotic) organellar genome trees of plants (Balbuena et al. 2013; Pérez-Escobar et al. 2016). It assesses phylogenetic congruence with the explicit goal of testing the dependence of one phylogeny on another, accommodating large-scale data and allowing for the examination of phylogenetic congruence between highly enriched clades (Hutchinson et al. 2017). Due to the high degree of intragenomic congruence of the Loliinae plastome-coding genes (Minaya et al. 2017; Moreno-Aguilar et al. 2020), whole plastome alignment was employed to generate 1000 bootstrap plastome trees. To do this, a phylogenetic reconstruction was carried out using IQ-TREE2, providing the program with partition information for each nuclear and plastome alignment, executing 1000 ultrafast bootstrap replicates and saving the respective bootstrap trees (ufboot). This procedure evaluates the similarities between any pair of topologies by comparing the Euclidean distances that separate the terminals in both trees through the Procrustean superposition (Balbuena et al. 2013). The sum of the squared residuals (the disparity between an observed value and a fitted value derived from a model) for each association and each pair of topologies evaluated can be interpreted as a concordance score because it is directly proportional to the magnitude of the topological conflict for the pair of terminals considered (Pérez-Escobar et al. 2016). Differences in terminal position between nuclear and plastome ML trees were summarized in bar plots using the R package *ggplot2* (Wickham 2016). The sum of squared residuals for each pair of nuclear and plastome gene terminals was classified into quartiles, and the magnitude of discordance was assessed by the proportion of genes binned in quartiles 3 and 4 (50% and 75%) in each terminal. The higher the number of genes binned in these quartiles, the greater the discordance is (Pérez-Escobar et al. 2021). Furthermore, we examined the congruence of nuclear versus plastome topologies using generalized Robinson-Foulds (gRF) distances, a metric that allows matching of similar splits in the compared trees, giving similarity scores to each pair of splits and the overall similarity measure. gRF distances were calculated for the Loliinae tree and for the major BL and FL lineages using the R package TreeDist, following Smith (2020) and Hendriks et al. (2023).

Due to the relatively high cytonuclear concordance detected for the main backbone Loliinae topologies, we dated the origins of the Loliinae lineages using the concatenated IQ-TREE2 ML phylogeny with branch length information and the treePL software (Smith and O'Meara 2012). We constrained four nodes of the tree using dates inferred from our previous studies. Three nodes were calibrated using secondary age constrains for the crown nodes of the BOP (Oryza + Pooideae) clade (normal prior maximum = 55.08, minimum = 47.76 Ma), Loliinae clade (normal prior maximum = 23.13, minimum = 16.02 Ma), BL Loliinae clade (normal prior maximum = 20.45, minimum = 12.15 Ma), and a fourth node was calibrated using a minimum age constrain for the crown node of FL Loliinae (lognormal prior maximum = 19.75, minimum = 14.13 Ma) based on a *Festuca* sect. *Festuca*

leaf macrofossil dated to the Early Miocene (Moreno-Aguilar et al. 2020). The analyses were performed using smoothing values of 0.1 to estimate the best optimization parameter values (3-3-5), which were then used in a subsequent analysis to calculate divergence times. Confidence intervals of nodal ages estimates were calculated from 1000 bootstrap replicates summarized in TreeAnnotator 2.7.7 (Bouckaert et al. 2014) (Supplementary Appendix 7).

Results

Sequencing Data, Nuclear Orthologous Single-Copy Gene Filtering, Plastome Data

On average, 2.95 M PE reads per sample, ranging from 1.29 M in *F. pyrenaica* to 8.64 M in *F. californica*, were generated for target capture data. The average recovery of reads per genus was similar for *Festuca* (3.05 M), *Vulpia* (3.35 M), *Wangenheimia* (3.31 M), *Micropyropsis* (3.69 M), and *Psilurus* (3.62 M), and slightly less for *Megalachne* (2.59 M) and *Lolium* (2.42 M) (Supplementary Table S1 and Supplementary Appendix 1). The total number of Loliinae nuclear target genes obtained from the Angiosperms353 kit was 352. The mean number of genes recovered by HybPiper with >50% of the target length for Loliinae samples across the entire sampling was 275, representing 77.95% of the target loci, whereas the mean number of genes with >75% of the target length was 193 (54.70%) (Supplementary Appendix 1). We obtained 270 MI single-copy genes (Supplementary Table S2 and Supplementary Appendix 3), and 184 MO genes, which contains 175 1-to-1 orthologs and 9 strict MO orthologs (Appendix 4). Because the ASTRAL-Pro topology computed from the 352-gene data set and the concatenated IQ-TREE2 ML trees and ASTRAL-III coalescent topologies computed from the filtered 270-gene (MI) and 184-gene (MO) data sets showed high agreement with each other (Figs. 1 and 2; Supplementary Fig. S3), we selected the MI data, which produced the phylogeny with the highest average posterior probability and bootstrap percentages, as the optimal Loliinae scg-strict data set, composed of 270 genes and 135 tips (132 Loliinae species plus three outgroups), representing, on average, 68.27% of the 353 reference genes. Alignments of individual single-copy nuclear genes ranged from 90 to 2217 bp, with a mean length of 677.04 bp (Supplementary Table S2 and Supplementary Appendix 3). The final alignment of 270 concatenated and partitioned nuclear genes for 132 Loliinae species in the scg-strict data set was 170,329 bp in length. The percentage of missing data was 13.74% and the percentage of parsimony informative sites 23.1% (39,275 bp) (see Supplementary Appendix 6). The number of "paralogs" retrieved by HybPhaser for the 132 Loliinae across the scg-inclusive data set ranged from 210 (*F. modesta*) to 269 (*F. andicola*), representing, respectively, 40.6% to 76.7% of the total (270 genes) (Supplementary Table S3).

Genome skimming data from 79 newly sequenced samples ranged from 1.56 M (*H. livida*) to 35.89 M (*F. glauca*) PE reads. The newly assembled complete plastomes ranged between 103,079 bp (*H. livida*) and 134,746 bp (*F. costata*), which is consistent with plastome length values obtained in previous studies of Loliinae for the respective FL and BL clades (Moreno-Aguilar, 2022a) (Supplementary Table S1 and Supplementary Appendix 5). Most of the newly assembled plastomes showed good read coverage (>40×). The MSA of the complete plastomes was 135,268 bp in length [18,225 (13.5%) variable sites, 7210 (5.3%) parsimony informative sites], with *H. livida*, *V. muralis*, and *P. incurvus* being the samples with the highest percentage of missing data (21.6%) (Supplementary Appendix 6).

Loliinae Nuclear Target Capture Phylogenies, Intragenomic Discordances, ILS/IH Signals, and Hybrid-Level Detection

Phylogenetic trees recovered from the Loliinae 270 scg-strict data set using supermatrix ML and MSC approaches are largely consistent in topology (Figs. 1 and 2; Supplementary Fig. S4). Both phylogenies supported the divergences of the major BL (Drymanthele-Phaeochloa + Scariosae + Lojaconoa + Pseudoscariosa; Tropical–South Africa; Subbulbosae + Leucopoa, Schedonorus-Lolium) and FL lineages (Eskia; American II; American-Neozeylandic; American I; Psilurus-Vulpia (px); Festuca + Wangenheimia; Afroalpine). However, the two trees showed different placement regarding the basal resolution of the BL clade (paraphyletic in the ML tree, monophyletic in the MSC tree) and in the inferred relationships of some BL (Mexico-Central American-South American [MCSA] I and II) and FL ("intermediate" Subulatae-Hawaiian; American-Vulpia Pampas; Loretia + Exaratae; Aulaxyper; Afroalpine (*F. caprina*) lineages) (Supplementary Fig. S4). The main topological discordances were related to the different placements of the BL MCSA I (Glabricarpae, Asperifolia, Drymanthele s. l.) and MCSA II (Erosiflorae, Ruprechtia, Coironhuecu) groups, resolved as basal paraphyletic lineages of the Subbulbosae-Leucopoa/Schedonorus clade in the ML tree (Fig. 1), but nested into two separate clades (Subbulbosae-Leucopoa, and Tropical-South Africa clade) in the MSC tree (Fig. 2; Supplementary Fig. S4). In both trees, all MSCA lineages descended from MSCA ancestors except *F. argentina* (Coironhuecu), which nested within the Subbulbosae + Leucopoa clade and was resolved as sister of *F. altaica* (Figs. 1 and 2). The Exaratae-Loretia group was divided into a clade ((*V. membranacea*/*V. sicula*), *F. plicata*) sister to Psilurus-Vulpia (px), and other lineages (*F. hephaestophila, F. capillifolia*/*F. pyrenaica*), which showed different relationships with Aulaxyper p.p. lineages and to Afroalpine or to American-Vulpia-Pampas, American I and Festuca in the ML and MSC trees (Figs. 1 and 2; Supplementary Fig. S4). Our large-scale sampling of taxa (Supplementary Table S1) enriched the phylogenetic circumscriptions of

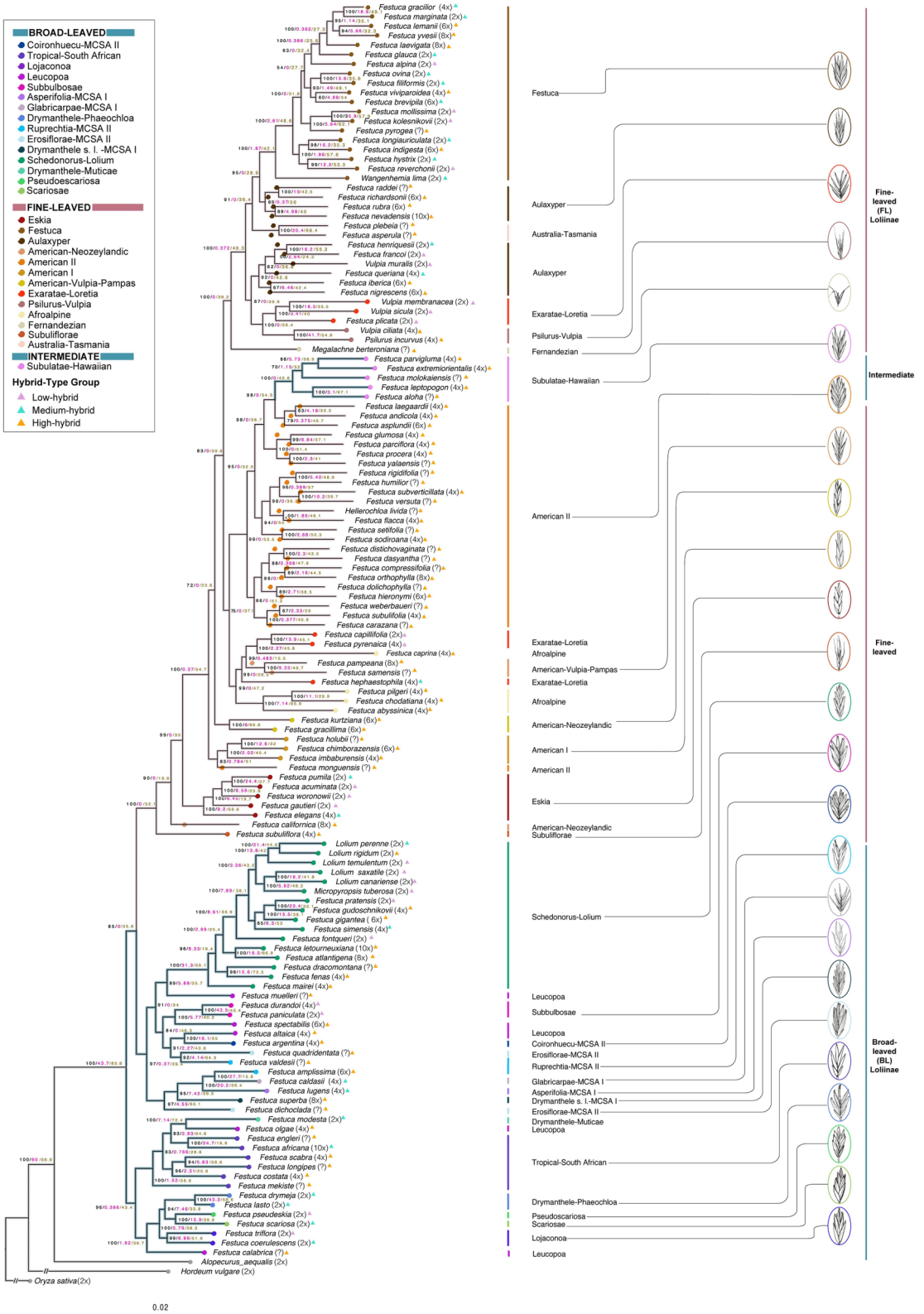

FIGURE 1. Maximum likelihood (ML) single-copy gene phylogeny of Loliinae constructed from a concatenated supermatrix (scg-strict data set) of 270 genes and 132 ingroup taxa. Numbers on branches indicate UltraFast Bootstrap support (BS, black), gene concordance factor (gCF, pink), and site concordance factor (sCF, brown) values (see Supplementary Table S4), respectively. Scale bar: number of mutations per site. Color codes of Loliinae lineages are indicated in the chart. Drawings of spikelets are shown for representative species of each Loliinae lineage. Drawings by M. F. Moreno-Aguilar.

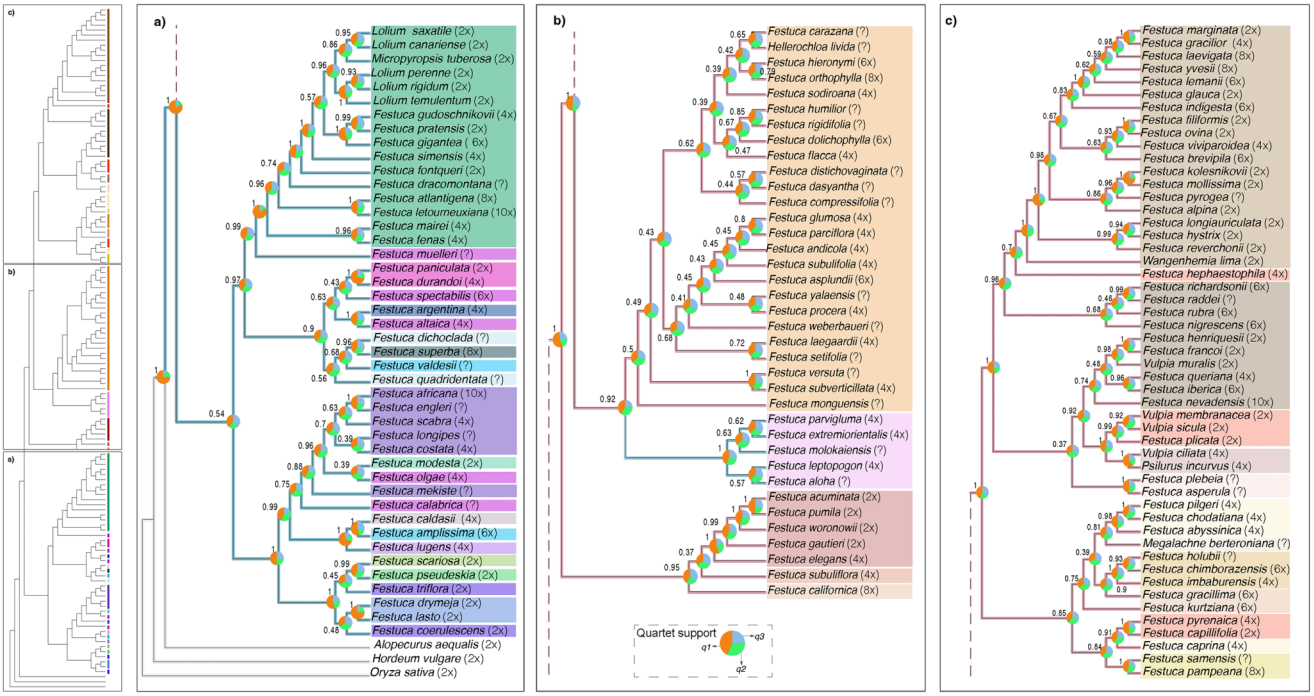

FIGURE 2. Multispecies Coalescent (MSC) ASTRAL species tree of 132 Loliinae taxa inferred from 270 ML single-copy gene trees (scg-strict data set). Numbers above branches show posterior probability support (PPS) values and below their consecutive numbering. Pie diagrams at nodes correspond to quartet support values for branches of the best tree and the alternative topologies (*q1*, *q2*, and *q3*; see color codes in the chart and Supplementary Table S5). *Oryza sativa* was used to root the trees. Color codes of Loliinae lineages correspond to those of Figure 1.

several clades or groups with newly studied species (Festuca: *F. gracilior*, *F. kolesnikovii*, *F. marginata*, *F. mollisima*, *F. reverchonii*, *F. yvesii*; Aulaxyper: *F. raddei*, *F. richardsonii*; Australia-Tasmania: *F. asperula*, *F. plebeia*; American-Vulpia-Pampas: *F. samensis*; American-Neozeylandic: *F. kurtziana*; American I: *F. imbaburensis*; American II: *F. carazana*, *F. dasyantha*, *F. distichovaginata*, *F. dolichophylla*, *F. glumosa*, *F. humilior*, *F. laegaardii*, *F. monguensis*, *F. procera*, *F. parciflora*, *F. rigidifolia*, *F. setifolia*, *F. sodiroana*, *F. subulifolia*, *F. versuta*, *F. weberbaueri*; Subulatae-Hawaiian: *F. leptopogon*; Eskia: *F. acuminata*, *F. woronovii*; Asperifolia: *F. lugens*). Most of these species clustered in the same groups in the ML and MSC trees, although their phylogenetic placements differed in some cases from tree to tree (Figs. 1 and 2; Supplementary Fig. S4). The strongly supported Australian *F. asperula*/*F. plebeia* clade (new 29th Loliinae lineage) was closely related to the Aulaxyper group, but constituted a separate Australia-Tasmania lineage of this grade in both trees (Figs. 1 and 2; Supplementary Fig. S4). The taxonomically and phenotypically diverse American II lineage included species classified within the FL *Hellerochloa* (*H. livida*) and *Festuca* sect. *Festuca* (e.g., *F. andicola*, *F. orthophylla*) or within different FL supraspecific *Festuca* ranks (e.g., *F. versuta* (*F.* subgen. *Drymanthele* sect. *Texanae*)/*F. subverticillata* (*F.* subgen. *Obtusae*), *F. flacca* (*F.* subgen. *Subulatae* sect. *Subulatae*)) (Supplementary Table S1), although they were all nested in the same clade in both trees. Our ML and MSC analyses indicate that *F. subverticillata* belongs to the American II clade whereas *F. hephaestophila* is not affiliated with the *Festuca* lineage but could be placed within the Exaratae grade (Figs. 1 and 2; Supplementary Fig. S4). The BL species *F. californica* (*F.* subgen. *Leucopoa* sect. *Breviaristatae*) and *F. subuliflora* (*F.* subgen. *Subuliflora*) were resolved as closely related species (Figs. 1 and 2) in the MSC and ML phylogenies, nesting in early divergent lineages within the FL clade. *Festuca muelleri* (*F.* subgen. *Drymanthele* sect. *Banksia*) was strongly resolved as a sister lineage to the Schedonorus-Lolium clade in both trees (Figs. 1 and 2). The Eurasian BL *F. modesta* (*F.* subgen. *Drymanthele* sect. *Muticae*) and *F. calabrica* and *F. olgae* (*F.* subgen *Leucopoa*), and the South African *F. mekiste* fell within an expanded Tropical-South African+ (plus) clade in the MSC tree, and all of them but *F. calabrica* (resolved as sister to Drymanthele-Phaeochloa + Scariosae + Lojaconoa + Pseudoscariosa) in the ML tree (Figs. 1 and 2; Supplementary Fig. S4).

Node support was high for most tree branches in both the ML (ultrafast median BS values mostly 100%) and MSC (most median PPS values close to 1) trees (Figs. 1 and 2). However, the mean percentages of gCF and sCF were medium-low, at 44.10% and 7.32%, respectively in the ML tree (Fig. 1; Supplementary Table S4). Similarly, genomic discordance between single-copy nuclear genes used to reconstruct the 270 scg-strict MSC phylogeny of Loliinae was high for most lineages (Fig. 2; Supplementary Table S5 and Supplementary Fig. S5).

The estimation of the proportion of gene tree quartets concordant with the ASTRAL species tree via normalized quartet scores indicated considerable intragenomic incongruence. The nodes of the MSC tree obtained values ranging from 33.76% to 82.83% for the main topology (*q1*); 8.90% to 40.55% for the first alternative topology (*q2*), and 7.66% to 39.81% for the second alternative topology (*q3*), but with a mean of only 42.78% across all nodes of the species tree (*q1*) (Supplementary Table S5). The highest intragenomic concordances were found for the crown nodes of Loliinae (81.32% for *q1*), Schedonorus-Lolium (82.83%), Drymanthele-Phaeochloa (75.67%) and Psilurus-Vulpia-px (60.71%) followed by the moderate concordance of those of Subbulbosae (71.96%), FL Loliinae *sensu lato* (including Subulatae-Hawaiian) (56.20%), and FL Eskia (56.2%), whereas the remaining lineages showed very low concordances (Fig. 2; Supplementary Table S5). These patterns suggest ILS as the primary driver of topological discordance; however, quantitative evaluation of ILS versus IH nodal indices indicated that other potential causes of discordance, such as introgression, could be causing the incongruence between the gene trees and species trees (Supplementary Fig. S5 and Supplementary Table S5). Phytop analysis revealed prominent ILS signatures (ILS-i, 24.47–99.35%) across the Loliineae lineages, and considerable introgression probabilities (IH-i, 10.28–49.7%) for 18 nodes, with the highest IH-i probabilities detected at divergence nodes N5 (BL clade, 49.7%), N9 (Eskia, 41.63%), N16 (American II + Subulatae-Hawaiian, 44.0%), N34 (Schedonorus-Lolium p.p., 42.0%), N43 (Festuca-Wangenheimia + Aulaxyper pp., 42.8%), N57 (Festuca + Wangenheimia, 48.7%), and N70 (Festuca, 38.4%) (Supplementary Fig. S5 and Supplementary Table S5).

To obtain more precise data on hybridization rates in specific Loliinae lineages, we analyzed the HybPhaser data of the scg-inclusive data set using all 269 saved alleles. Estimations of the proportion of LH and of AD over all available genes per sample indicated that, although some samples (35) showed low range values, corresponding to non-hybrids or low-hybrid levels (LH < 82.4%; AD < 1.7), others (97) displayed medium- or high-hybrid signatures (Fig. 3 a,b; Supplementary Fig. S6 and Supplementary Table S3). Within the latter two classes, we were able to separate 87 samples as high hybrids and 10 as medium hybrids (Fig. 3a,b; Supplementary Table S3 and Supplementary Fig. S6). This low-medium-high hybrid-level classification matched well the diploid-tetraploid-high ploidy levels and ancestral-to-recent evolutionary histories of the studied taxa but with some exceptions (Supplementary Table S3). Afroalpine (100%), American-Neozeylandic (100%), American-Vulpia-Pampas (100%), American I (100%), American II (100%), Aulaxyper p.p. (60%), Australia-Tasmania (100%), Drymanthele s.l. (100%), Drymanthele-Muticae (100%), Erosiflorae (100%), Fernandezian (100%), Leucopoa (80%), Psilurus-Vulpia (100%), Subulatae-Hawaiian (100%), Subuliflorae (100%), Coironhuecu (100%), and Tropical-South African p.p. (66.6%) were the Loliinae lineages richest in high-hybrid taxa, consistent with their high ploidy levels and relatively recent origins, whereas Asperifolia (100%) and Glabricarpae (100%) had medium hybrid levels, in line with their tetraploid genomes. In contrast, Drymanthele-Phaeochloa (100%), Eskia (100%), Exaratae-Loretia p.p. (71.4%), Lojaconoa (100%), Pseudoscariosa (100%), Scariosae (100%), and Subbulbosae (100%) were the least hybrid lineages, in accordance with their predominantly diploid levels and evolutionary ancestry. Festuca and Schedonorus-Lolium displayed a relatively balanced representation of low and high hybrid levels (Festuca: 42.1% and 42.1%; Schedonorus-Lolium: 37.5% and 50%), with Festuca also displaying medium hybrid levels (15.8%) each fitting their corresponding diploid-tetraploid-high ploidy levels and ancestral-intermediate-recent origins (Fig. 3a,b; Supplementary Fig. S6 and Supplementary Table S3).

Evidence of Widespread Reticulation, Gene Duplications, and Allopolyploidizations in Loliinae

Species network analysis supported widespread reticulate evolution in Loliinae (Fig 4a; Supplementary Fig. S7 and Supplementary Table S6). Phylonet analysis and the AICc and BIC criteria suggested a complex network of 10 reticulations as the best-fitting scenario of all models analyzed, although the best-fit reticulation scenario may not have been reached. Notably, however, the four scenarios with the highest probabilities and lowest AICc and BIC scores (7, 8, 9, and 10 reticulations) inferred a hybrid origin for FL lineages from ancestral parental BL lineages or their derived FL hybrid lineages (Supplementary Fig. S7). The optimal scenario supported a hybrid origin for core lineages of the FL clade (Exaratae-Loretia, Aulaxyper, Festuca) from unknown ancestral and Leucopoa-type BL parental lineages, for basal FL lineages (Eskia) from subbasal BL lineages and the core FL clade, and for intermediately evolved FL lineages from different combinations of BL and FL parental lineages (Subulatae-Hawaiian, American II, Afroalpine) or from hybrid FL parental lineages (American-Neozeylandic, American I). Reticulated origins for basal and subbasal BL lineages (Leucopoa p.p., MCSA) were also inferred from other lineages in nearby clades (Fig. 4a).

Both Notung analyses (i.e., one based on 302 gene trees from the scg-full data set and the other based on 167 filtered gene trees from scg-full data set that have an average BS higher than 60) identified 14 branches of the MSC tree of Loliinae with proportions of duplicated genes greater than 10% (Fig. 4b; Supplementary Table S7). We described here the result of those based on the 302 gene trees data set. The highest proportions were

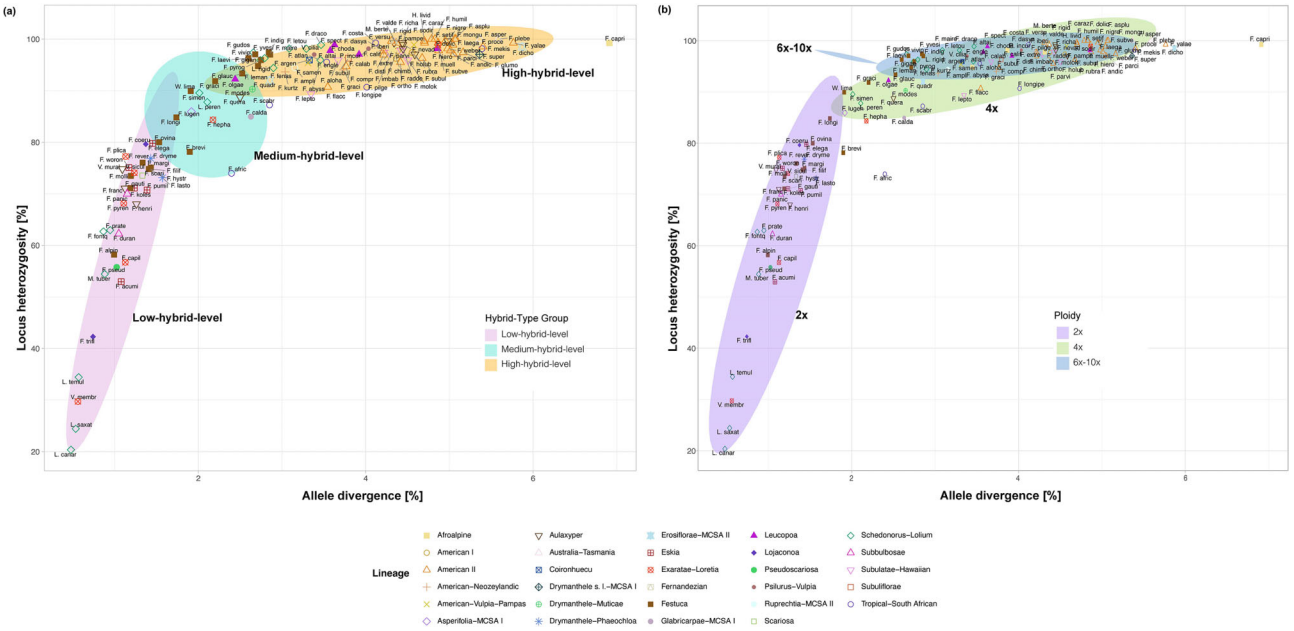

FIGURE 3. Scatterplots displaying the locus heterozygosity (LH) and allele divergence (AD) values of the studied Loliinae samples retrieved from HybPhaser (see Supplementary Table S3). (a) Colored ellipses indicate three main hybrid classes: i) low hybrid level (low-to-medium LH (≥10–≤82.4) and low AD (>0–≤1.7)); ii) medium hybrid level (medium LH (≥70–< 90) and medium AD (>1.71–≤2.8)); and iii) high hybrid level (high LH (≥80) and high AD (>2.8)). (b) Color codes for ploidy levels of samples: i) diploids (2x), ii) tetraploids (4x), and iii) high-polyploids (≥6x). Color codes for hybrid classes and ploidy levels and symbols for Loliinae lineages are indicated in the respective charts.

those of the subcore FL clade (N10, 0.519), followed by the Schedonorus-Lolium lineage (N22, 0.43), the core FL clade (N28, 0.31) and the FL (N6, 0.26) and BL (N5, 0.21) clades. Some of these duplications correspond to clades with many confirmed allopolyploid taxa, such as those in the Schedonorus-Lolium group, and others specific to ancestral nodes, such as the BL and FL (total, subcore, core) clades, could correspond to early WGD events (Fig. 4b). When we used GRAMPA to investigate the nature of these duplications, the program yielded the lowest parsimony scores for MUL trees for 14 nodes, indicating allopolyploidization scenarios for all these nodes have better reconciliation scores than the singly labeled species tree scenarios (Fig. 4b; Supplementary Fig. S8).

Plastome Phylogeny of Loliineae

The strongly supported plastome ML tree (Supplementary Fig. S9) was generally consistent with the single-copy nuclear gene ML tree in the placement of major BL and FL clades (Fig. 1; Supplementary Fig. S10), although the composition and the relationships between some lineages within these clades differed. In the plastome BL clade, most of the MCSA taxa plus South African *F. scabra* and *F. longipes* and Eurasian *F. calabrica* formed a sister clade to the remaining BL taxa. Within this last clade, successive splits separated the lineages Lojaconoa-Pseudoscariosa, Drymanthele (Phaeochloa)-Scariosae, Tropical-South African (plus *F. olgae*), Subbulbosae-Leucopoa (plus *F. valdesii*), and Schedonorus-Lolium. In the plastome FL (*sensu lato*) clade, the "intermediate" American-Neozeylandic lineage (*F. californica*/*F. gracillima*) split first, followed by those of Subuliflorae + Leucopoa (Breviaristatae) (*F. altaica*) + Eskia p.p. I (*F. acuminata*/*F. pumila*), and Eskia p.p. II (*F. elegans*, *F. gautieri*, *F. woronowii*) + American I + American II p.p. (*F. monguensis*, *F. parciflora*, *F. kurtziana*). The divergence of two sister clades followed, one including the successive splits of the American-Vulpia-Pampas/Fernandezian, Psilurus-Vulpia(px), the Exaratae-Loretia grade, and Subulatae-Hawaiian lineages, and the other the Festuca-Wangenheimia, Aulaxyper-Vulpia (2x), and American II + Afroalpine lineages (Supplementary Fig. S9).

Divergence Time Estimation Analysis

Our penalized likelihood divergence time analysis performed on the single-copy nuclear gene ML tree (Fig. 5) provided age estimates for the stem and crown Loliinae nodes dating to the Late-Oligocene (25.02 Ma) and Early Miocene (18.81 Ma), respectively. Early-to-Mid-Miocene divergences were inferred for the BL (16.87 and 16.48 Ma) and FL (16.14 Ma) ancestors, and Mid-Miocene-to-Late-Miocene ages for those of the more recently evolved BL [Drymanthele-Phaeochloa + Lojaconoa + Scariosae + Pseudoscariosa + Leucopoa (*F. calabrica*) (13.99 Ma), Tropical-South Africa + Drymanthele-Muticae + Leucopoa (*F. olgae*) (14.02 Ma), MCSA (13.41 Ma), MCSA II + Sub-

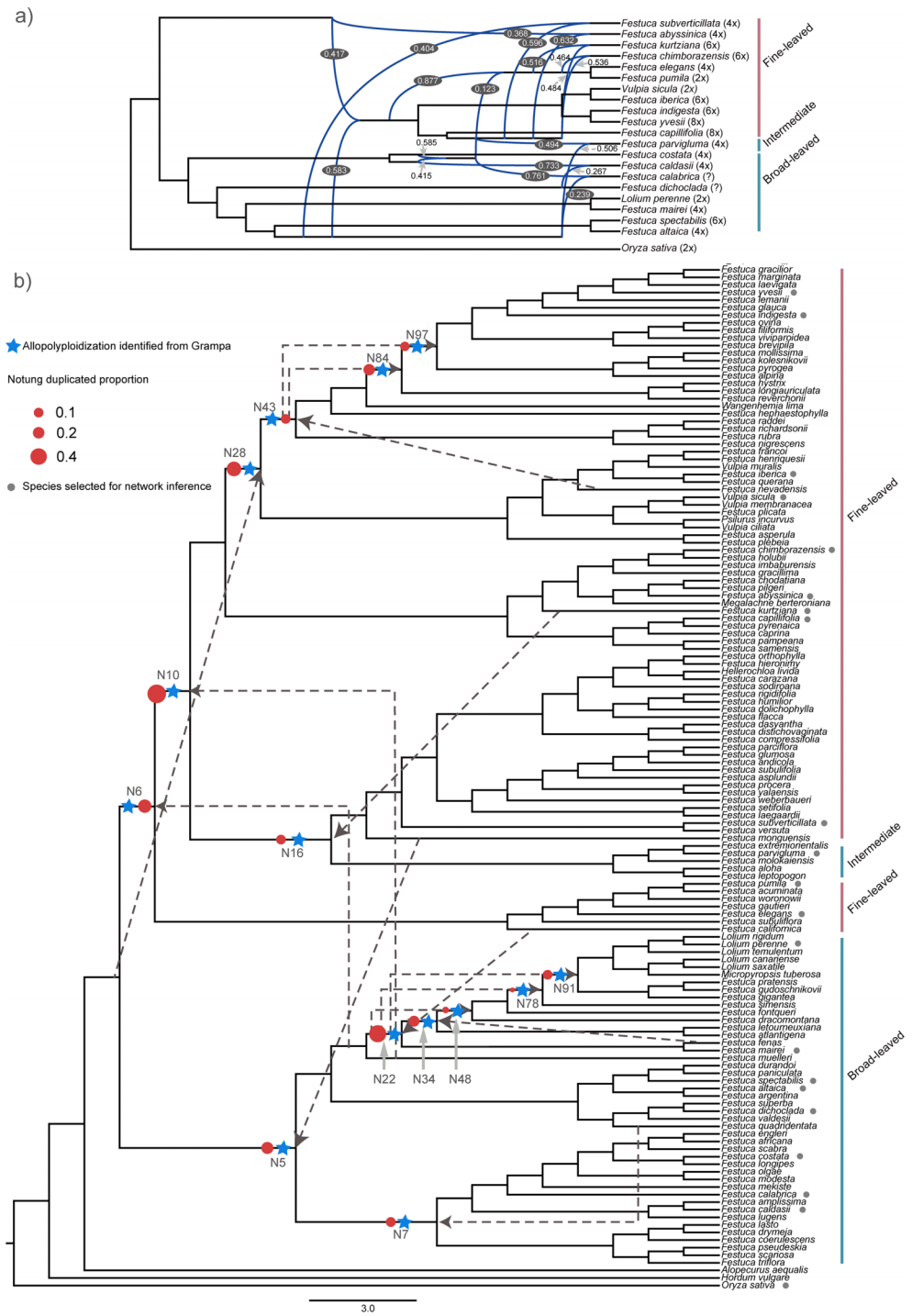

FIGURE 4. (a) Phylogenetic network of the reduced 20-taxon data set representing the major lineages of Loliinae plus *Oryza sativa* as the outgroup, inferred by PhyloNet using maximum pseudo-likelihood under the best-fit 10-reticulation model scenario supported by AICc and BIC (see Supplementary Fig. S7 and Supplementary Table S6). The blue branches indicate contributions of the lineages involved in the reticulated histories, and the values next to or on top of it indicate the inferred inheritance probability. (b) Gene duplications mapped over the Loliinae tree and inference of allopolyploid events. Proportions of duplicated genes estimated by Notung for branches of the Loliinae topology (red dots) mapped on the MSC tree (see Supplementary Table S7); size of red dots indicates the proportion of duplicated genes (see chart), only duplications >0.10 are indicated. The blue stars correspond to the 14 allopolyploidization events inferred by GRAMPA in the BL and FL clades of Loliinae; all of these scenarios were supported by the lowest parsimony (reconciliation) scores compared with the highest scores of the non-WGD scenarios in the GRAMPA tests (see Supplementary Fig. S8). The dashed lines connect the second putative parental lineage to each allopolyploid. The 21 taxa selected for network inference (see Fig. 4a) are indicated with a gray circle.

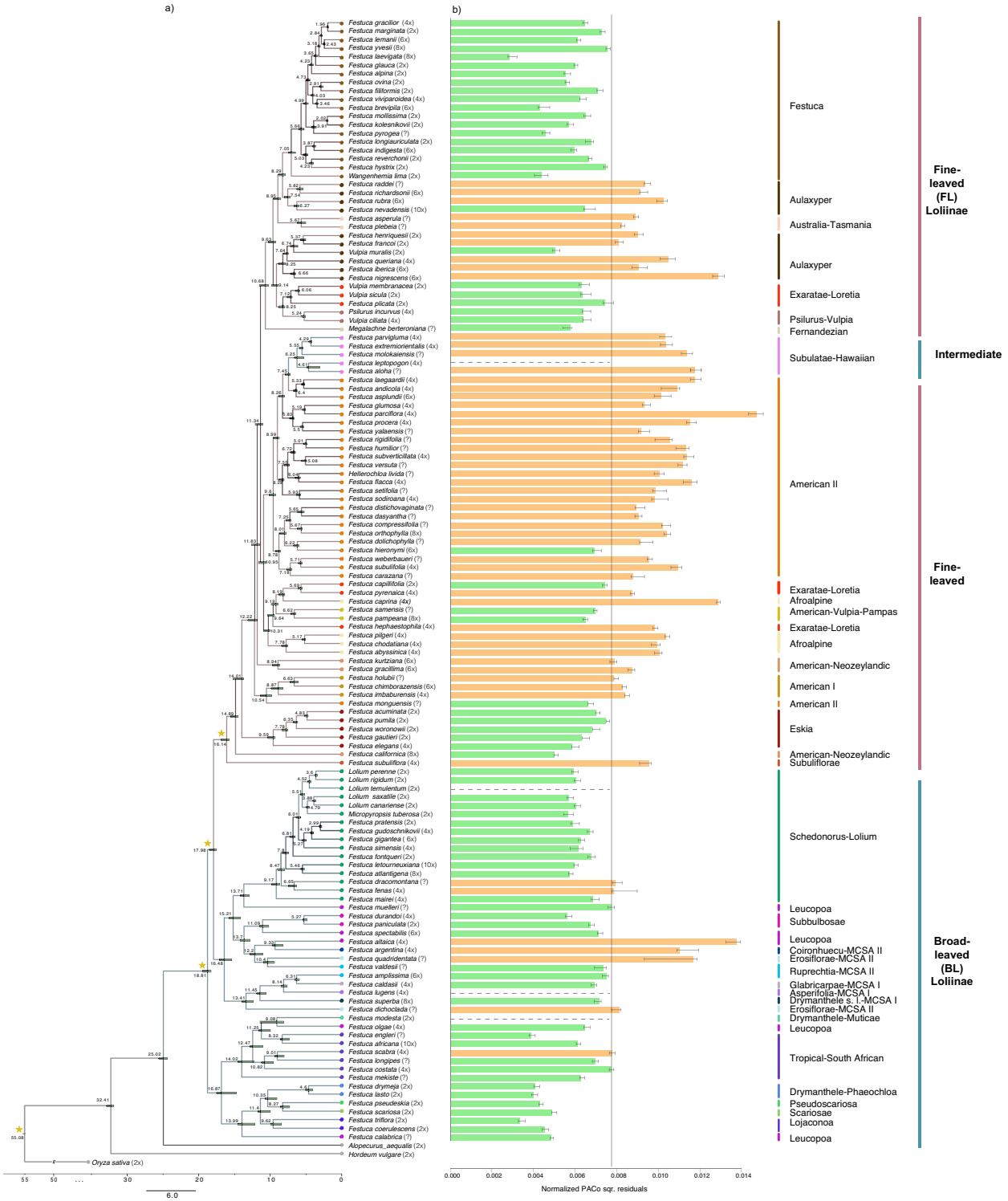

FIGURE 5. (a) Maximum penalized likelihood dated tree constructed with TreePL using the ML single-copy gene phylogeny of Loliinae obtained from a concatenated supermatrix of 270 genes and 132 taxa and four calibrations. Nodal values show the inferred divergence ages; stars indicate the calibrated nodes. Confidence intervals of time estimates were calculated from 1000 bootstrap replicates. (b) Boxplot showing PACo normalized squared residual values obtained from 1000 random replicates of nuclear-plastome associations. The horizontal black line equals $1/n = 0.0077$, where $n = 128$ is the number of common nuclear-plastome terminal associations; median values above this threshold are expected to be linked to species that show incongruence between nuclear and plastome-derived trees (orange boxes) whereas values below the threshold correspond to topologically congruent species (green boxes) (see also Supplementary Fig. S7).

bulbosae + Leucopoa (13.7 Ma), Schedonorus (9.17 Ma)] and FL [American-Neozeylandic (*F. californica*) (14.89 Ma), Eskia (9.59 Ma), American I + American II (*F. monguensis*) (10.54 Ma), American-Neozeylandic (8.94 Ma), Afroalpine + American-Vulpias-Pampas + Exaratae-Loretia p. p. (10.31 Ma), American II (9.6 Ma), Subulatae-Hawaiian (6.25 Ma), Fernandezian (10.68 Ma), Exaratae-Loretia p.p. + Psilurus-Vulpia (8.25 Ma), Aulaxyper-Vulpia (8.25–7.54 Ma), Australian-Tasmania (5.67 Ma), Festuca-Wangenheimia (7.05 Ma)] lineages (Fig. 5).

Cytonuclear Topological Incongruence Assessments

Topological incongruence analysis performed using PACo on the single-copy nuclear gene ML trees versus plastome ML gene trees suggested 56 terminals as potentially conflicting (Fig. 1; Supplementary Figs. S9 and S10). The squared residual values of these terminals, calculated individually for each nuclear gene tree and with 46% of their values assigned to quartiles 3 and 4, were generally higher compared with 67 non-conflicting terminals (Fig. 5; Supplementary Fig. S6).

Our cytonuclear discordance assessments using gRF distances were performed for the entire Loliinae tree and for nine lineages with more than three shared species. The results showed a median gRF value of relatively high concordance for the Loliinae (0.3082), whereas those for specific lineages ranged from relatively high to moderate concordance [Schedonorus-Lolium (gRF = 0.3202), Tropical-South African (0.3075), Exarateae-Loretia (0.4200), Eskia (0.4897), Festuca (0.5206)] to increasing levels of discordance [Aulaxyper (0.6248), Leucopoa (0.7734), American II (0.8058)] (Supplementary Table S8).

Discussion

Utility of Single-Copy Nuclear Genes for Phylogenetic Analyses in Loliinae and Plant Systematics

Our phylogenomic analyses provide the first evolutionary reconstruction of Loliinae based on hundreds of nuclear-coding loci and offer a detailed case study of how large target capture data sets perform in a highly reticulate, polyploid-rich plant lineage (Figs. 1 and 2; Supplementary Figs. S4 and S10). Using 270 orthologous single-copy nuclear genes from the scg strict data set, we recovered a well-resolved backbone phylogeny that strongly supports the monophyly of Loliinae and the early divergence of its two major evolutionary lineages, BL and FL Loliinae. These relationships are recovered with high resolution and strong support in the concatenated ML tree (Fig. 1). The inferred topology is largely congruent with plastome-based phylogenies (Supplementary Figs. S9, S10) and with earlier studies based on a limited number of nuclear and plastid markers (Inda et al. 2008; Díaz Pérez et al., 2014; Minaya et al. 2015, Minaya et al. 2017), as well as analyses based on nuclear repetitive elements (Moreno-Aguilar et al. 2022b). Together, these results demonstrate that genome-wide nuclear data sets can robustly recover deep and intermediate divergences even in groups characterized by extensive hybridization and polyploidy, and that nuclear and organellar genomic compartments reconstruct a largely congruent evolutionary scenario for the major lineages of Loliinae. This congruence provides a solid framework for testing phylogenetic and statistical hypotheses about lineage origins and evolutionary processes within the subtribe.

Despite the overall robustness of the inferred backbone relationships, branch support decreases and several relationships differ between ancestral clades and more recently evolved BL and FL sublineages in the multispecies coalescent species tree inferred from single-copy nuclear genes (Fig. 2). The topological incongruences observed between the concatenated partitioned ML tree and the MSC species tree are more evident in the youngest Loliinae groups, such as the BL MCSA lineages and the FL American II taxa (Figs. 1, 2, and 5; Supplementary Fig. S4). These discrepancies are associated with extensive intragenomic discordance, as reflected by the distribution of the quartet scores across the MSC tree. Specifically, the quartets support values for the main topology of the MSC species tree range from moderate to high (33.76–82.83%) relative to those of the first and second alternative topologies (Fig. 2; Supplementary Table S5). For several of the ingroup nodes, the main topology accounts for the highest proportion of quartet support (mean $q1 = 42.78\%$), indicating that a majority of gene trees are concordant with the species tree. In contrast, other nodes exhibit nearly equal support among the three alternative topologies ($q1 \approx q2 \approx q3 \approx 0.33$), reflecting a near-random distribution of gene tree topologies (Fig. 2; Supplementary Table S5).

These patterns indicate that many internal branches in the Loliinae phylogeny have lengths close to zero, resulting in effective polytomies that cannot be fully resolved even with the 270 single-copy loci. Part of this extensive intragenomic discordance can be attributed to ILS (Stull et al. 2023), particularly in recently evolved Loliinae lineages that likely diverged during the Late Pliocene to Quaternary, as inferred from conservative divergence time estimates (Fig. 5; Minaya et al. 2017; Moreno-Aguilar et al. 2020). However, our quantitative assessments indicate that ILS alone does not account for the observed levels and patterns of discordance. Instead, the MSC phylogeny reveals substantial signals of reticulate evolution superimposed on pervasive ILS. ILS was identified as the predominant source of topological conflict for most incongruent nodes in the Loliinae phylogeny, affecting 96 nodes, with ILS indices ranging from 24.47% to 99.35%. At the same time, quantifiable introgression and hybridization contributed significantly to topological incongruences for 18 lineages, with

particularly high introgression indices detected in the BL clade as a whole (49.7%) and in the Schedonorus-Lolium lineage (42.0%), as well as in several FL lineages, including Festuca + Wangenheimia (48.7%), Festuca-Wangenheimia + Aulaxyper pp. (42.8%), Eskia (41.63%), American II + Subulatae-Hawaiian (40.87%), and Festuca (38.4%) (Supplementary Fig. S5; Supplementary Table S5).

Although the conserved and predominantly single-copy nuclear gene set of Angiosperms353 has proven to be an invaluable tool for reconstructing phylogenetic relationships at supraspecific levels in plants (Baker et al. 2021, Baker et al. 2022; Zuntini et al. 2024), its resolving power at the species and intraspecific levels remains variable. Some studies have demonstrated that these loci can resolve complex relationships in recently evolved lineages (Thomas et al. 2021), whereas others have emphasized substantial challenges associated with short internal branches, long branch attraction, and introgression in rapidly radiating groups (Maurin et al. 2021). In extreme cases, even thousands of nuclear orthologous genes have failed to recover strong quartet support for species in young, highly hybrid groups, such as Brassicaceae, due to pervasive intragenomic discordance (Züst et al. 2020), or have required the exclusion of most gene trees that are incongruent with diploid backbone phylogenies, as in *Brachypodium* (Sancho et al. 2022). Our results are consistent with these findings and with broader theoretical expectations (Philippe et al. 2011; Maurin et al. 2021), indicating that simply increasing the number of single-copy genes does not guarantee resolution in recently radiated and hybrid rich plant lineages.

Nevertheless, our analyses also show that careful gene selection, rigorous orthology assessment, and the combined use of concatenation and coalescent-based approaches can recover biologically meaningful phylogenetic signal despite high levels of intragenomic discordance (Smith et al. 2020). In Loliinae, the main topologies inferred from both concatenated partitioned ML and MSC consistently recover clades that correspond closely to established taxonomic circumscriptions and geographic distributions of species (Figs. 1 and 2; Supplementary Fig. S5; Catalán 2006; Catalán et al. 2007; Minaya et al. 2017; Moreno-Aguilar, 2022a). These results highlight the value of integrative phylogenomic frameworks for disentangling complex evolutionary histories and emphasize that conflict itself can be an informative signal of the processes shaping diversification in reticulate plant lineages.

Rampant Introgressions and Allopolyploidizations Framed the Evolutionary History of the Loliinae

Resolving the phylogeny of Loliinae is particularly challenging because most of its lineages have undergone multiple hybridization and allopolyploidization events. This complexity is supported by the medium to high hybridization levels, frequent gene duplications, and repeated allopolyploidy inferences detected across both BL and FL lineages in our analyses (Figs. 3 and 4; Supplementary Figs. S6 and S7), in agreement with previous records for the group (Catalán 2006; Moreno-Aguilar et al. 2022b). Divergence times obtained using treePL indicate that the main diversification within crown Loliinae occurred during the Early-to-Middle Miocene, giving rise to the BL and FL lineages. The inferred age of this split, approximately 18.81 Ma (Fig. 5a), closely matches previous estimates (Minaya et al. 2017; Moreno-Aguilar et al. 2020). Similarly, divergence times inferred for the main BL and FL clades show limited variation, with estimated ages of approximately 16.87 and 16.48 for BL lineages and 16.14 Ma for FL lineages (Fig. 5).

Despite this general temporal congruence, our analyses recovered differences in age estimates for several internal lineages, which are likely attributable to the larger number of nuclear genes analyzed here and the inclusion of newly sampled species. Examples include the Festuca clade, dated from approximately 7.05 to 1.96 Ma, and the American II clade, dated from approximately 9.6 to 5.01 Ma (Fig. 5a). This expanded data set increases phylogenetic resolution and provides a more robust temporal framework for interpreting lineage diversification. In addition, the accelerated radiation of species within Loliinae, particularly in the FL clade, emerges as a key evolutionary feature and appears to be closely associated with pronounced ploidy diversity and the proliferation of recently evolved lineages such as Festuca, Aulaxyper, and American II (Figs. 3a,b and 5a; Supplementary Table S1).

The pervasive nature of introgression in Loliinae is further supported by complementary analyses based on nuclear data and cytonuclear discordance. Medium to high levels of hybridization were detected across the subtribe through consistently high percentages of LH exceeding 70% and AD values exceeding 1.7% for the same set of nuclear genes across samples (Fig. 3a,b; Supplementary Fig. S6). A clear association emerges between low hybridization levels and ancestral diploids, intermediate hybridization levels and moderately evolved tetraploids, and high hybridization levels and recently evolved high polyploids. These putative hybrid taxa are distributed across multiple Loliinae lineages (Fig. 3a,b), although their frequency varies markedly among groups (Supplementary Fig. S6).

The complex reticulate scenario inferred from the best-fitting Loliinae species network (Fig. 4a; Supplementary Fig. S7) provides strong evidence that hybridization played a crucial role in the diversification of the subtribe. The inferred hybrid origin of all FL lineages, mainly from BL ancestors, is consistent with previous hypotheses proposing that more slender and recently evolved FL originated from more robust BL ancestors through reductions in genome and chromosome size accompanied by phenotypic changes (Catalán

2006; Šmarda et al. 2008; Moreno-Aguilar et al. 2022b), although the functional significance of these processes remains unresolved. In contrast, the putative hybrid origin of certain BL lineages, particularly the polyploid Leucopoa p.p. and the MSCA lineage, may be linked to long-distance dispersal events and the ecological adaptability of BL and FL ancestors in distinct paleobiogeographic contexts, as well as to the high propensity for hybridization and polyploidization among Southern Hemisphere Loliinae species (Minaya et al. 2017).

The inclusion of both slender and robust species within strongly supported FL lineages such as the American II clade, which encompasses taxa classified into disparate subgenera (Supplementary Table S1), further supports the interpretation of extensive hybrid swarming within this group (Moreno-Aguilar et al. 2020; Moreno-Aguilar, 2022a). Evidence for shared WGD events across multiple BL and FL lineages, together with corroborated allopolyploid origins of the BL, FL, and Schedonorus-Lolium groups (Fig. 4b; Supplementary Table S7), aligns with earlier hypotheses of post-allopolyploid diploidization in ancestral BL lineages such as Drymanthele and Phaeochloa. These hypotheses were originally inferred from genome size evolution, repetitive element dynamics, nuclear ribosomal DNA families, and the pronounced two-fold difference in genome size between these BL and FL diploids (Moreno-Aguilar et al. 2022b). Our results are also consistent with the genetically confirmed allopolyploid nature of key forage species within the Schedonorus-Lolium lineage (Kopecký and Studer 2014; Minaya et al. 2015) and several lineages of the core FL clade (Díaz-Pérez et al. 2014). Whether FL ancestors also acted as reciprocal progenitors in allopolyploidization events involving homologous BL lineages (Fig. 4b), which show similar inferred ages (Fig. 5), remains unresolved and will require further genomic investigation.

Cytonuclear incongruence analyses using PACo and gRF distance, together with quantitative comparisons of ILS and hybridization effects, further support the hybrid nature of 56 terminals that show strong but conflicting support in nuclear and plastid trees (Fig. 5; Supplementary Figs. S9 and S10). These terminals include lineages with both progenitors evolving within the BL clade (Subulatae-Hawaiian, Tropical-South African, MCSA) or FL clade (American II, Aulaxyper, Afroalpine, American-Neozeylandic), as well as "transclade" species derived from distantly related BL and FL ancestors, exemplified by *F. altaica*. In contrast, the most topologically congruent lineages across nuclear and plastid phylogenies include BL Schedonorus-Lolium, Subbulbosae, Drymanthele (Phaeochloa) and Lojaconoa, and FL Eskia, Festuca + Wangenheimia and American-Vulpia-Pampas groups (Fig. 5; Supplementary Figs. S9 and S10). Many of the discordant terminals correspond to polyploid taxa (Figs. 3 and 5; Supplementary Fig. S6 and Supplementary Table S1), further reinforcing the pervasive role of allopolyploidy in shaping Loliinae evolution, a pattern also supported by the strongly asymmetric karyotypes reported for several of these taxa (Martínez-Segarra et al. 2021; Moreno-Aguilar et al. 2022b).

Comparative analyses of nuclear LH and AD (LH-vs.-AD) hybrid classes with cytonuclear PACo and gRF discordance measures across Loliinae reveal a broadly correlated trend. Diploid and ancient polyploid species that are topologically congruent across nuclear and plastid trees generally show absent to low hybridization levels, as observed in BL Drymanthele-Phaeochloa, Lojaconoa, Scariosa, and Pseudoscariosa and FL Psilurus-Vulpia. In contrast, high-ploidy species exhibiting strong topological discordance typically display high hybridization levels, as observed in BL Coironhuecu and FL Afroalpine, American II, and Subulatae-Hawaiian (Fig. 3a,b; Supplementary Fig. S6). Several Loliinae groups show internally consistent but variable LH-versus-AD and PACo patterns, ranging from low hybridization levels and congruent topologies in diploids and tetraploids to high hybridization levels and incongruence in hexa-to-deca-polyploids (e.g., BL Tropical-South Africa p.p., FL Festuca p.p., Aulaxyper p.p., and the Exaratae-Loretia grade). However, some exclusively polyploid lineages present hybrid yet topologically congruent taxa, such as the BL MCSA I group and the FL American I, America-Vulpia-Pampas, and Fernandezian groups (Fig. 3a,b; Supplementary Fig. S6).

Notably, we did not detect a consistent relationship between hybridization levels or cytonuclear discordance and divergence time or shared ancestry within Loliinae (Fig. 5a,b). Sister or closely related lineages of comparable age often show contrasting patterns, as illustrated by the congruent American I and American-Vulpia-Pampas lineages dated from approximately 8.87 to 6.62 Ma, compared with the incongruent American II lineage dated from approximately 9.66 Ma. Similarly, the recently evolved FL Festuca lineage dated at approximately 7.05 million years and the Aulaxyper lineage dated from approximately 8.25 to 7.54 million years show markedly different patterns, with high polyploids of Aulaxyper exhibiting higher LH, AD, and cytonuclear discordance than those of Festuca (Figs. 3a,b and 5; Supplementary Fig. S6). Conversely, the BL Schedonorus-Lolium lineage, dated at approximately 9.17 Ma and encompassing a wide range of ploidy levels from diploids to decaploids, shows relatively low to moderate hybridization levels and no detectable topological discordance, even in well-known allopolyploids such as *F. arundinacea* and *F. letourneuxiana*. (Figs. 3a,b and 5a,b; Supplementary Fig. S6).

Taken together, these results suggest that evolutionary isolation and hybrid interactions are the primary drivers of the heterogeneous hybridization patterns observed in Loliinae. Species of the phylogenetically isolated Schedonorus-Lolium lineage have hybridized extensively among closely related taxa but

rarely with members of other lineages (Kopecký and Studer 2014; Glombik et al. 2021), explaining their high cytonuclear congruence. In contrast, within the large and phylogenetically non-isolated FL lineages, species of the Festuca clade have formed hybrid swarms and increased ploidy levels primarily through interactions with closely related taxa, resulting in relatively low cytonuclear discordance (Catalán 2006). By contrast, the highly cross-compatible hexaploid Aulaxyper taxa (*Festuca* sect. *Aulaxyper*) readily hybridize both within and across FL clades and even with other FL genera such as *Vulpia* (= *Festulpia*) (Catalán 2006; Catalán et al. 2007), leading to pronounced topological discordance (Figs. 3a,b and 5a,b; Supplementary Fig. S6).

The high proportion of allopolyploid species in Loliinae, representing approximately 70% of samples with known ploidy levels (Supplementary Table S1), likely exacerbated overall phylogenetic discordance. Fully resolving the evolutionary histories of orphan allopolyploids will ultimately require whole-genome or transcriptome-scale data (Sancho et al. 2022), which are currently lacking for most Loliinae lineages. Although we do not claim to have reconstructed the complete evolutionary history of Loliinae, the combined analysis of nuclear single-copy genes and plastome data presented here reveals critical patterns of hybridization and polyploidization that have shaped diversification across the subtribe and provides a framework for future genomic investigations.

Interpreting the Loliinae Reticulated Scenario within a Broad Angiosperm Evolutionary Framework

The reticulate evolutionary history inferred for Loliinae in this study closely parallels patterns reported for other hybrid-rich and allopolyploid angiosperm lineages of comparable diverging ages (Perez-Escobar et al., 2016; Morales-Briones et al. 2018, 2021; Sanderson et al. 2023; Hendriks et al. 2023; Stull et al. 2023), including several closely related grass lineages within Pooideae (Marcussen et al. 2015; Glémin et al. 2019; Zhang et al. 2022, Zhang et al. 2024). Despite this growing body of evidence, the relative contributions of deep versus recent hybridization and allopolyploidization events to diversification in Loliinae and other Pooideae remain incompletely resolved. Phylotranscriptomic and comparative genomic studies have revealed multiple gene duplication events in Pooideae lineages, including duplications involving genes associated with vernalization, cold tolerance, ecological adaptation, and spikelet development (Zhang et al. 2022, Zhang et al. 2024). In addition to the ancient WGD inferred for the protograss ancestor (Zhang et al. 2024), the existence of a more recent paleopolyploid ancestor for Loliinae could not be excluded. This possibility is supported by the inference of allopolyploidization events in the ancestors of both BL and FL Loliinae clades based on our GRAMPA analyses (Fig. 4b), as well as by evidence for multiple WGDs at the crown nodes of closely related Poeae lineages such as *Poa*, *Deschampsia*, and *Agrostis* (Zhang et al. 2022).

The detection of ancient allopolyploidization signatures, however, is complicated by rapid genomic rearrangements involving gene gains and losses and by the superposition of successive hybridization events (Stull et al. 2023). Resolving these complex evolutionary histories also depends critically on dense taxonomic sampling, as exemplified by the *Triticum-Aegylops* complex, where extensive hybridization has made the origins of polyploid wheat genomes difficult to disentangle. In that system, multiple alternative scenarios involving ancient and recent homoploid hybridization and allopolyploidization among different genome donor taxa continue to be debated to explain the origins of the B and D subgenomes of polyploid wheats (Marcussen et al. 2015; Glémin et al. 2019). In this context, the extensive sampling of Loliinae lineages in our study, combined with integrated nuclear and plastome-based phylogenomic analyses, provides a robust framework for detecting and interpreting hybridization and allopolyploidization processes within the subtribe.

Although divergence time estimates suggest that the origins of the BL and FL Loliinae lineages were nearly contemporaneous (Fig. 5a), our results indicate that the Early-to-Middle Miocene BL ancestors were slightly older than the FL ancestor. Additional lines of evidence support the interpretation of early diverging BL Loliinae lineages as ancient hybrids or paleo-allopolyploids sensu Stull et al. (2023), in which gene flow has ceased and genomes have subsequently stabilized. In contrast, FL Loliinae lineages, particularly those within the core FL clade, appear to represent more recent meso- or neo-allopolyploids characterized by high genomic diversity (Figs. 4 and 5). Consistent with this interpretation, our Notung analyses revealed higher gene duplication rates in FL clades than in BL clades, with the exception of the recently evolved Schedonorus-Lolium lineage. Moreover, GRAMPA inferred allopolyploidization events in BL lineages primarily involving outgroups or other BL lineages, whereas basal FL lineages show clear signals of allopolyploid origin from BL ancestors (Fig. 4b).

Inheritance probabilities estimated from the Loliinae phylogenetic network further support different hybridization scenarios in the two major clades, a pattern also observed in other angiosperms (Molero-Briones et al. 2018). The asymmetric, and especially the low contributions (<0.3), from alternative BL parental populations to reticulated BL nodes are consistent with introgression among stabilized lineages. By contrast, the predominantly symmetric inheritance probabilities close to 0.5 observed for reticulated FL nodes strongly support recent allopolyploidization and hybrid speciation events involving BL ancestors (Fig. 4a). These network-based results corroborate cytogenomic evidence for ancestral diploidization processes in early diverging BL lineages inferred from repeatome composition and nuclear ribosomal DNA analyses (Moreno-Aguilar et al. 2022b).

They are also consistent with the pronounced reductions in chromosome number and monoploid genome size observed from diploid BL to FL lineages (Catalán, 2006; Šmarda et al. 2008; Moreno-Aguilar et al. 2022b), which likely facilitated the emergence of progenitor species that later participated in recent FL allopolyploidization events (Fig. 4).

Cytonuclear discordance and discordance between nuclear gene trees have been used to detect ancient and recent hybridization and allopolyploidization in plants (Perez-Escobar et al., 2016; Morales-Briones et al. 2018, 2021; Hendriks et al. 2023; Sanderson et al. 2023; Stull et al. 2023). Our exploratory analyses of cytonuclear incongruence in Loliinae lineages using PACo, together with assessments of hybridization classes based on LH and AD metrics, revealed clear contrasts between BF and FL lineages. Most BL lineages exhibit high cytonuclear concordance, whereas most FL lineages show low concordance, regardless of their inferred hybridization class (Figs. 3 and 5b; Supplementary Fig. S6). These contrasting patterns further support a scenario of older and more stabilized allopolyploid histories in BL Loliinae compared with the more recent and dynamic allopolyploid evolution of FL lineages. The divergent cytonuclear patterns observed in the recently evolved and closely related Festuca and Aulaxyper lineages are particularly informative. Despite potentially sharing common BL ancestors (Figs. 4 and 5), Festuca taxa exhibit relatively high cytonuclear congruence, whereas Aulaxyper taxa show pronounced incongruence. These differences are likely explained by contrasting propensities for hybridization, with Festuca species primarily interbreeding within their own clade and Aulaxyper species hybridizing more frequently both within and beyond their clade (Catalán 2006). These contrasting hybridization tendencies are not associated with differences in life cycle or mating system (Mitchell and Whitney 2021; Stull et al. 2023), as species in both groups are perennial and predominantly outcrossing (Catalán 2006; Catalán et al. 2007). Notably, highly polyploid Aulaxyper taxa readily hybridize not only with perennial congeners but also with diploid and polyploid annual species of *Vulpia* (FL Aulaxyper and Exaratae-Loretia lineages) and occasionally with distantly related diploid *Lolium* species (BL Schedonorus-Lolium lineage) (Catalán 2006). The demonstrated ability of hexaploid Aulaxyper species to eliminate excess repetitive elements from their genomes (Moreno-Aguilar et al. 2022b) may facilitate such wide hybridization by reducing genomic incompatibilities and stabilizing interspecific and intergeneric hybrids.

Together, these results place the Loliinae within a broader angiosperm framework in which ancient stabilized allopolyploidy, recurrent recent hybridization, and lineage specific differences in cross compatibility interact to shape long-term evolutionary trajectories. Fully testing these hypotheses and resolving the genomic mechanisms underlying these processes will require comprehensive whole-genome analyses, which remain largely unavailable for Loliinae. Nonetheless, the phylogenomic framework presented here provides a critical foundation for understanding reticulate evolution across grasses and flowering plants more generally.

Acknowledgments

We thank the editors, Drs. Isabel Sanmartin, Robert C. Thomson, and Tiina Särkinen, and four anonymous reviewers for their valuable comments that greatly improved the manuscript, the AAU, HUTPL, OSC, MO, CONC, US, UZ, and VBGI herbaria for lending Loliinae samples for our study, the Ministerio del Ambiente of Ecuador for permitting us to collect Loliinae samples in the Ecuadorian páramos (MAEDNB-CM-2015-0016), and Dr. Luis A. Inda for his advice on ploidy levels of Loliinae. Target capture data and genome skimming data of the studied samples were generated at Arbor Biosciences (Ann Arbor, USA) and at the Centro Nacional de Análisis Genómicos (CNAG, Barcelona, Spain) and Macrogen (Madrid, Spain), respectively. The bioinformatic and evolutionary analyses were performed in the Bioflora laboratory of the Escuela Politécnica Superior de Huesca (Universidad de Zaragoza, Spain).

Author Contributions

P.C., M.F.M.-A., and J.V. designed the study. M.F.M.-A., J.C.O., G.M.-S., J.A.D., I.A., W.C., A.S., and P.C. collected the samples. M.F.M.-A.and C.C. developed the experimental work. M.F.M.-A., C.C., J.V., A.S.-R., D.C., I.A., and P.C. analyzed the data and interpreted the results. P.C. and M.F.M.-A. wrote the draft manuscript. All authors have read and agreed to the published version of the manuscript.

Supplementary Material

Supplementary material is available at *Systematic Biology* online.

Conflict of Interest

The authors declare no conflict of interest.

Funding

This study was supported by the Spanish Ministry of Science and Innovation PID2022-140074NB-I00 and the Spanish Aragon Government and European Social Fund Bioflora A01-23R research grants. M.F.M.-A. was supported by a University of Zaragoza-Santander Ph.D. fellowship. C.C. was funded by a University of Zaragoza postdoctoral contract and J.V. by RYC2023-042611-I and MCIU/AEI/10.13039/501100011033 grants.

Data Availability

All the original data and scripts necessary to reproduce the analyses reported in this study can be accessed through the Dryad link: https://doi.org/10.5061/dryad.4xgxd25pn

References

Baker W.J., Bailey P., Barber V., Barker A., Bellot S., Bishop D., Botigué L.R., Brewer G., Carruthers T., Clarkson J.J., Cook J., Cowan R.S., Dodsworth S., Epitawalage N., Françoso E., Gallego B., Johnson M.G., Kim J.T., Leempoel K., Maurin O., McGinnie C., Pokorny L., Roy S., Stone M., Toledo E., Wickett N.J., Zuntini A.R., Eiserhardt W.L., Kersey P.J., Leitch I.J., Forest F. 2022. A comprehensive phylogenomic platform for exploring the angiosperm tree of life. Syst. Biol. 71(2):301–319.

Baker W.J., Dodsworth S., Forest F., Graham S.W., Johnson M.G., McDonnell A., Pokorny L., Tate J.A., Wicke S., Wickett N.J. 2021. Exploring angiosperms353: an open, community toolkit for collaborative phylogenomic research on flowering plants. Am. J. Bot. 108(7):1059–1065.

Balbuena J.A., Míguez-Lozano R., Blasco-Costa I. 2013. PACo: a novel procrustes application to cophylogenetic analysis. PLoS One 8(4):e61048.

Bankevich A., Nurk S., Antipov D., Gurevich A.A., Dvorkin M., Kulikov A.S., Lesin V.M., Nikolenko S.I., Pham S., Prjibelski A.D., Pyshkin A.V., Sirotkin A.V., Vyahhi N., Tesler G., Alekseyev M.A., Pevzner P.A. 2012. SPAdes: a new genome assembly algorithm and its applications to single-cell sequencing. J. Comput. Biol. 19(5):455–477.

Bolger A.M., Lohse M., Usadel B. 2014. Trimmomatic: a flexible trimmer for Illumina sequence data. Bioinformatics 30(15):2114–2120.

Borowiec M.L. 2016. AMAS: a fast tool for alignment manipulation and computing of summary statistics. PeerJ 4:e1660.

Bouckaert R., Heled J., Kühnert D., Vaughan T., Wu C.-H., Xie D., Suchard M.A., Rambaut A., Drummond A.J. (2014) BEAST 2: A Software Platform for Bayesian Evolutionary Analysis. PLoS Comput Biol 10(4):e1003537. https://doi.org/10.1371/journal.pcbi.1003537

Brown J.W., Walker J.F., Smith S.A. 2017. Phyx: phylogenetic tools for unix. Bioinformatics 33(12):1886–1888.

Capella-Gutiérrez S., Silla-Martínez J.M., Gabaldón T. 2009. trimAl: a tool for automated alignment trimming in large-scale phylogenetic analyses. Bioinformatics 25(15):1972–1973.

Catalán P. 2006. Phylogeny and evolution of *Festuca* L. and related genera of subtribe Loliinae (Poeae, Poaceae). In: Sharma A.K., Sharma A., editors. Plant genome: biodiversity and evolution. Enfield (NH): Science Publishers. p.255–303.

Catalán P., Torrecilla P., López-Rodríguez J., Müller J., Stace C. 2007. A systematic approach to subtribe Loliinae (Poaceae: Pooideae) based on phylogenetic evidence. Aliso 23(1):380–405.

Catalán P., Torrecilla P., Rodríguez J.Á.L., Olmstead R.G. 2004. Phylogeny of the festucoid grasses of subtribe Loliinae and allies (Poeae, Pooideae) inferred from ITS and trnL-F sequences. Mol. Phylogenet. Evol. 31(2):517–541.

Chen K., Tang Z.-J., Wang Y., Tan J.-B., Zhou S.-D., He X.-J., Xie D.-F. 2025. Phylogenomic analyses reveal species relationships and phylogenetic incongruence with new member detected in allium subgenus cyathophora. Plants 14(13):2083.

Cui X., Li E., He J., Wang Y., Shang C., Zhong B., Viruel J., Dong W., Zhang Z. 2025. Ancient hybridization drives arid adaptation and species diversification in Caragana (Fabaceae). New Phytol. 247(5):2454–2472.

Díaz-Pérez A.J., Sharifi-Tehrani M., Inda L.A., Catalán P. 2014. Polyphyly, gene-duplication and extensive allopolyploidy framed the evolution of the ephemeral *Vulpia* grasses and other fine-leaved Loliinae (Poaceae). Mol. Phylogenet. Evol. 79:92–105.

Dierckxsens N., Mardulyn P., Smits G. 2017. NOVOPlasty: de novo assembly of organelle genomes from whole genome data. Nucleic Acids Res. 45:e18.

Dubcovsky J., Martínez A. 1992. Distribución geográfica de los niveles de ploidía en Festuca. Parodiana 7:91–99.

Dunning L.T., Olofsson J.K., Parisod C., Choudhury R.R., Moreno-Villena J.J., Yang Y., Dionora J., Quick W.P., Park M., Bennetzen J.L., Besnard G., Nosil P., Osborne C.P., Christin P.-A. 2019. Lateral transfers of large DNA fragments spread functional genes among grasses. Proc. Natl. Acad. Sci. USA 116(10):4416–4425.

Emms D.M., Kelly S. 2015. OrthoFinder: solving fundamental biases in whole genome comparisons dramatically improves orthogroup inference accuracy. Genome Biol. 16(1):157.

Glémin S., Scornavacca C., Dainat J., Burgarella C., Viader V., Ardisson M., Sarah G., Santoni S., David J., Ranwez V. 2019. Pervasive hybridizations in the history of wheat relatives. Sci. Adv. 5: eaav9188.

Glombik M., Copetti D., Bartos J., Stoces S., Zwierzykowski Z., Ruttink T., Wendel J.F., Duchoslav M., Dolezel J., Studer B., Kopecky D. 2021. Reciprocal allopolyploid grasses (Festuca × Lolium) display stable patterns of genome dominance. Plant J. 107(4):1166–1182.

Hendriks K.P., Kiefer C., Al-Shehbaz I.A., Bailey C.D., Hooft van Huysduynen A., Nikolov L.A., Nauheimer L., Zuntini A.R., German D.A., Franzke A., Koch M.A., Lysak M.A., Toro-Núñez Ó., Özüdoğru B., Invernón V.R., Walden N., Maurin O., Hay N.M., Shushkov P., Mandáková T., Schranz M.E., Thulin M., Windham M.D., Rešetnik I., Španiel S., Ly E., Pires J.C., Harkess A., Neuffer B., Vogt R., Bräuchler C., Rainer H., Janssens S.B., Schmull M., Forrest A., Guggisberg A., Zmarzty S., Lepschi B.J., Scarlett N., Stauffer F.W., Schönberger I., Heenan P., Baker W.J., Forest F., Mummenhoff K., Lens F. 2023. Global Brassicaceae phylogeny based on filtering of 1,000-gene dataset. Curr. Biol. 33(19):4052–4068.e6.

Hoang D.T., Chernomor O., von Haeseler A., Minh B.Q., Vinh L.S. 2018. UFBoot2: improving the ultrafast bootstrap approximation. Mol. Biol. Evol. 35(2):518–522.

Huber K.T., Oxelman B., Lott M., Moulton V. 2006. Reconstructing the evolutionary history of polyploids from multilabeled trees. Mol. Biol. Evol. 23(9):1784–1791.

Hutchinson M.C., Cagua E.F., Balbuena J.A., Stouffer D.B., Poisot T. 2017. Methods Ecol. Evol. 8(8):932–940.

Inda L.A., Segarra-Moragues J.G., Müller J., Peterson P.M., Catalán P. 2008. Dated historical biogeography of the temperate Loliinae (Poaceae, Pooideae) grasses in the northern and southern hemispheres. Mol. Phylogenet. Evol. 46(3):932–957.

Johnson M.G., Gardner E.M., Liu Y., Medina R., Goffinet B., Shaw A.J., Zerega N.J.C., Wickett N.J. 2016. HybPiper: extracting coding sequence and introns for phylogenetics from high-throughput sequencing reads using target enrichment. Appl. Plant Sci. 4(7):1600016.

Johnson M.G., Pokorny L., Dodsworth S., Botigué L.R., Cowan R.S., Devault A., Eiserhardt W.L., Epitawalage N., Forest F., Kim J.T., Leebens-Mack J.H., Leitch I.J., Maurin O., Soltis D.E., Soltis P.S., Wong G.K.S., Baker W.J., Wickett N.J. 2019. A universal probe set for targeted sequencing of 353 Nuclear genes from any flowering plant designed using k-medoids clustering. Syst. Biol. 68(4):594–606.

Junier T., Zdobnov E.M. 2010. The Newick utilities: high-throughput phylogenetic tree processing in the UNIX shell. Bioinformatics 26(13):1669–1670.

Kalyaanamoorthy S., Minh B.Q., Wong T.K., von Haeseler A., Jermiin L.S. 2017. ModelFinder: fast model selection for accurate phylogenetic estimates. Nat. Methods 14(6):587–589.

Katoh K., Standley D.M. 2013. MAFFT multiple sequence alignment software version 7: improvements in performance and usability. Mol. Biol. Evol. 30(4):772–780.

Keuler R., Garretson A., Saunders T., Erickson R.J., St. Andre N., Grewe F., Smith H., Lumbsch H.T., Huang J.-P., St. Clair L.L., Leavitt S.D. 2020. Genome-scale data reveal the role of hybridization in lichen-forming fungi. Sci. Rep. 10(1):1497.

Koenen E.J.M., Ojeda D.I., Bakker F.T., Wieringa J.J., Kidner C., Hardy O.J., Pennington R.T., Herendeen P.S., Bruneau A., Hughes C.E. 2021. The origin of the legumes is a complex paleopolyploid phylogenomic tangle closely associated with the cretaceous-paleogene (K-Pg) mass extinction event. Syst. Biol. 70(3):508–526.

Kopecký D., Studer B. 2014. Emerging technologies advancing forage and turf grass genomics. Biotechnol. Adv. 32(1):190–199.
Li H., Handsaker B., Wysoker A., Fennell T., Ruan J., Homer N., Marth G., Abecasis G., Durbin R. 2009. The sequence alignment/map format and SAMtools. Bioinformatics 25(16):2078–2079.
Liu L., Anderson C., Pearl D., Edwards S.V. 2019. Modern phylogenomics: building phylogenetic trees using the multispecies coalescent model. Methods Mol. Biol. 1910:211–239.
Mandáková T., Lysak M.A. 2018. Post-polyploid diploidization and diversification through dysploid changes. Curr. Opin. Plant Biol. 42:55–65.
Marcussen T., Heier L., Brysting A.K., Oxelman B., Jakobsen K.S. 2015. From gene trees to a dated allopolyploid network: insights from the angiosperm genus *Viola* (Violaceae). Syst. Biol. 64(1):84–101.
Martínez-Sagarra G., Castro S., Mota L., Loureiro J., Devesa J.A. 2021. Genome size, chromosome number and morphological data reveal unexpected infraspecific variability in *Festuca* (Poaceae). Genes 12(6):906.
Maurin O., Anest A., Bellot S., Biffin E., Brewer G., Charles-Dominique T., Cowan R.S., Dodsworth S., Epitawalage N., Gallego B., Giaretta A., Goldenberg R., Gonçalves D.J.P., Graham S., Hoch P., Mazine F., Low Y.W., McGinnie C., Michelangeli F.A., Morris S., Penneys D.S., Pérez Escobar O.A., Pillon Y., Pokorny L., Shimizu G., Staggemeier V.G., Thornhill A.H., Tomlinson K.W., Turner I.M., Vasconcelos T., Wilson P.G., Zuntini A.R., Baker W.J., Forest F., Lucas E. 2021. A nuclear phylogenomic study of the angiosperm order Myrtales, exploring the potential and limitations of the universal Angiosperms353 probe set. Am. J. Bot. 108(7):1087–1111.
Minaya M., Díaz-Pérez A., Mason-Gamer R., Pimentel M., Catalán P. 2015. Evolution of the beta-amylase gene in the temperate grasses: non-purifying selection, recombination, semiparalogy, homeology and phylogenetic signal. Mol. Phylogenet. Evol. 91:68–85.
Minaya M., Hackel J., Namaganda M., Brochmann C., Vorontsova M.S., Besnard G., Catalán P. 2017. Contrasting dispersal histories of broad- and fine-leaved temperate Loliinae grasses: range expansion, founder events, and the roles of distance and barriers. J. Biogeogr. 44(9):1980–1993.
Minh B.Q., Hahn M.W., Lanfear R. 2020. New methods to calculate concordance factors for phylogenomic datasets. Mol. Biol. Evol. 37(9):2727–2733.
Minh B.Q., Schmidt H.A., Chernomor O., Schrempf D., Woodhams M.D., von Haeseler A., Lanfear R. 2020. IQ-TREE 2: new models and efficient methods for phylogenetic inference in the genomic era. Mol. Biol. Evol. 37(5):1530–1534.
Mitchell N., Whitney K.D. 2021. Limited evidence for a positive relationship between hybridization and diversification across seed plant families. Evolution 75:1966–1982.
Morales-Briones D.F., Kadereit G., Tefarikis D.T., Moore M.J., Smith S.A., Brockington S.F., Timoneda A., Yim W.C., Cushman J.C., Yang Y. 2021. Disentangling sources of gene tree discordance in phylogenomic data sets: testing ancient hybridizations in Amaranthaceae sl. Syst. Biol. 70(2):219–235.
Morales-Briones D.F., Liston A., Tank D.C. 2018. Phylogenomic analyses reveal a deep history of hybridization and polyploidy in the Neotropical genus *Lachemilla* (Rosaceae). New Phytol. 218(4):1668–1684.
Moreno-Aguilar M.F., Arnelas I., Sánchez-Rodríguez A., Viruel J., Catalán P. 2020. Museomics unveil the phylogeny and biogeography of the neglected Juan Fernandez Archipelago Megalachne and Podophorus endemic grasses and their connection with relict Pampean-Ventanian Fescues. Front. Plant Sci. 11:1–18.
Moreno-Aguilar M.F., Inda L.A., Sánchez-Rodríguez A., Arnelas I., Catalán P. 2022. Evolutionary dynamics of the repeatome explains contrasting differences in genome sizes and hybrid and polyploid origins of grass Loliinae lineages. Front. Plant Sci. 13:901733.
Moreno-Aguilar M.F., Inda L.A., Sánchez-Rodríguez A., Catalán P., Arnelas I. 2022. Phylogenomics and systematics of overlooked Mesoamerican and South American polyploid broad-leaved festuca grasses differentiate F. sects. Glabricarpae and Ruprechtia and F. subgen. Asperifolia, Erosiflorae, Mallopetalon and Coironhuecu (subgen. nov.). Plants 11(17): 2303.
Nauheimer L., Weigner N., Joyce E., Crayn D., Clarke C., Nargar K. 2021. HybPhaser: a workflow for the detection and phasing of hybrids in target capture data sets. Appl. Plant Sci. 9(7):e11441.
Nguyen L.-T., Schmidt H.A., von Haeseler A., Minh B.Q. 2015. IQ-TREE: a fast and effective stochastic algorithm for estimating maximum-likelihood phylogenies. Mol. Biol. Evol. 32(1):268–274.
Pérez-Escobar O.A., Balbuena J.A., Gottschling M. 2016. Rumbling orchids: how to assess divergent evolution between chloroplast endosymbionts and the nuclear host. Syst. Biol. 65(1): 51–65.
Pérez-Escobar O.A., Dodsworth S., Bogarín D., Bellot S., Balbuena J.A., Schley R.J., Kikuchi I.A., Morris S.K., Epitawalage N., Cowan R., Maurin O., Zuntini A., Arias T., Serna-Sánchez A., Gravendeel B., Torres Jimenez M.F., Nargar K., Chomicki G., Chase M.W., Leitch I.J., Forest F., Baker W.J. 2021. Hundreds of nuclear and plastid loci yield novel insights into orchid relationships. Am. J. Bot. 108(7): 1166–1180.
Philippe H., Brinkmann H., Lavrov D.V., Littlewood D.T.J., Manuel M., Wörheide G., Baurain D. 2011. Resolving difficult phylogenetic questions: why more sequences are not enough. PLoS Biol. 9(3): e1000602.
Sancho R., Inda L.A., Díaz-Pérez A., Des Marais D.L., Gordon S., Vogel J.P., Lusinska J., Hasterok R., Contreras-Moreira B., Catalán P. 2022. Tracking the ancestry of known and "ghost" homeologous subgenomes in model grass *Brachypodium* polyploids. Plant J. 109(6):1535–1558.
Sanderson B.J., Gambhir D., Feng G., Hu N., Cronk Q.C., Percy D.M., Freaner F.M., Johnson M.G., Smart L.B., Keefover-Ring K., Yin T., Ma T., DiFazio S.P., Liu J., Olson M.S. 2023. Phylogenomics reveals patterns of ancient hybridization and differential diversification that contribute to phylogenetic conflict in willows, poplars, and close relatives. Syst. Biol. 72(6):1220–1232.
Schwarz G. 1978. Estimating the dimension of a model. Ann. Statist. 6(2):461–464.
Shang H.Y., Jia K.H., Li N.W., Zhou M.J., Yang H., Tian X.L., Ma P.F., Zhang R.G. 2025. Phytop: a tool for visualizing and recognizing signals of incomplete lineage sorting and hybridization using species trees output from ASTRAL. Hortic. Res. 12(3):uhae330
Šmarda P., Bureš P., Horová L., Foggi B., Rossi G. 2008. Genome size and GC content evolution of Festuca: ancestral expansion and subsequent reduction. Ann. Bot. 101:421–433.
Smith M.R. 2020. Information theoretic generalized Robinson–Foulds metrics for comparing phylogenetic trees. Bioinformatics 36(20):5007–5013.
Smith S.A., O'Meara B.C. 2012. treePL: divergence time estimation using penalized likelihood for large phylogenies. Bioinformatics 28(20):2689–2690.
Smith S.A., Walker-Hale N., Walker J.F., Brown J.W. 2020. Phylogenetic conflicts, combinability, and deep phylogenomics in plants. Syst. Biol. 69(3):579–592.
Soltis D.E., Visger C.J., Marchant D.B., Soltis P.S. 2016. Polyploidy: pitfalls and paths to a paradigm. Am. J. Bot. 103(7):1146–1166.
Stolzer M., Lai H., Xu M., Sathaye D., Vernot B., Durand D. 2012. Inferring duplications, losses, transfers and incomplete lineage sorting with nonbinary species trees. Bioinformatics 28(18):i409–i415.
Stull G.W., Pham K.K., Soltis P.S., Soltis D.E. 2023. Deep reticulation: the long legacy of hybridization in vascular plant evolution. Plant J. 114(4):743–766.
Sugiura N. 1978. Further analysts of the data by Akaike' s information criterion and the finite corrections. Commun. Stat. Theory Methods. 7(1):13–26
Than C., Ruths D., Nakhleh L. 2008. PhyloNet: a software package for analyzing and reconstructing reticulate evolutionary relationships. BMC Bioinf. 9(1):322.
Thomas A.E., Igea J., Meudt H.M., Albach D.C., Lee W.G., Tanentzap A.J. 2021. Using target sequence capture to improve the phylogenetic resolution of a rapid radiation in New Zealand Veronica. Am. J. Bot. 108(7):1289–1306.
Thomas G.W.C., Ather S.H., Hahn M.W. 2017. Gene-tree reconciliation with MUL-trees to resolve polyploidy events. Syst. Biol. 66(6):1007–1018.

Wen D.Q., Yu Y., Zhu J.F., Nakhleh L. 2018. Inferring phylogenetic networks using PhyloNet. Syst. Biol. 67(4):735–740.
Wickham H. 2016. ggplot2: Elegant graphics for data analysis. New York: Springer-Verlag.
Yang L., Harris A.J., Wen F., Li Z., Feng C., Kong H., Kang M. 2023. Phylogenomic analyses reveal an allopolyploid origin of core Didymocarpinae (Gesneriaceae) followed by rapid radiation. Syst. Biol. 72(5):1064–1083.
Yang Y., Smith S.A. 2014. Orthology inference in nonmodel organisms using transcriptomes and low-coverage genomes: improving accuracy and matrix occupancy for phylogenomics, Mol. Biol. Evol. 31(11):3081–3092.
Yu Y., Nakhleh L. 2015. A maximum pseudo-likelihood approach for phylogenetic networks. BMC Genomics 16(S10):S10.
Zhang C., Nielsen R., Mirarab S. 2025. ASTER: a package for large-scale phylogenomic reconstructions. Mol. Biol. Evol. 42(8):1–4.
Zhang C., Scornavacca C., Molloy E.K., Mirarab S. 2020. ASTRAL-Pro: quartet-based species-tree inference despite paralogy. Mol. Biol. Evol. 37(11):3292–3307.
Zhang L., Zhu X., Zhao Y., Guo J., Zhang T., Huang W., Huang J., Hu Y., Huang C.H., Ma H. 2022. Phylotranscriptomics resolves the phylogeny of Pooideae and uncovers factors for their adaptive evolution. Mol. Biol. Evol. 39(2):msac026.
Zhang T., Huang W., Zhang L., Li D.Z., Qi J., Ma H. 2024. Phylogenomic profiles of whole-genome duplications in Poaceae and landscape of differential duplicate retention and losses among major Poaceae lineages. Nat. Commun. 15(1):3305.
Zuntini A.R., Carruthers T., Maurin O., Bailey P.C., Leempoel K., Brewer G.E., Epitawalage N., Françoso E., Gallego-Paramo B., McGinnie C., Negrão R., Roy S.R., Simpson L., Toledo Romero E., Barber V.M.A., Botigué L., Clarkson J.J., Cowan R.S., Dodsworth S., Johnson M.G., Kim J.T., Pokorny L., Wickett N.J., Antar G.M., DeBolt L., Gutierrez K., Hendriks K.P., Hoewener A., Hu A.Q., Joyce E.M., Kikuchi I., Larridon I., Larson D.A., de Lírio E.J., Liu J.X., Malakasi P., Przelomska N.A.S., Shah T., Viruel J., Allnutt T.R., Ameka G.K., Andrew R.L., Appelhans M.S., Arista M., Ariza M.J., Arroyo J., Arthan W., Bachelier J.B., Bailey C.D., Barnes H.F., Barrett M.D., Barrett R.L., Bayer R.J., Bayly M.J., Biffin E., Biggs N., Birch J.L., Bogarín D., Borosova R., Bowles A.M.C., Boyce P.C., Bramley G.L.C., Briggs M., Broadhurst L., Brown G.K., Bruhl J.J., Bruneau A., Buerki S., Burns E., Byrne M., Cable S., Calladine A., Callmander M.W., Cano Á., Cantrill D.J., Cardinal-McTeague W.M., Carlsen M.M., Carruthers A.J.A., de Castro Mateo A., Chase M.W., Chatrou L.W., Cheek M., Chen S., Christenhusz M.J.M., Christin P.A., Clements M.A., Coffey S.C., Conran J.G., Cornejo X., Couvreur T.L.P., Cowie I.D., Csiba L., Darbyshire I., Davidse G., Davies N.M.J., Davis A.P., van Dijk K.J., Downie S.R., Duretto M.F., Duvall M.R., Edwards S.L., Eggli U., Erkens R.H.J., Escudero M., de la Estrella M., Fabriani F., Fay M.F., Ferreira P.L., Ficinski S.Z., Fowler R.M., Frisby S., Fu L., Fulcher T., Galbany-Casals M., Gardner E.M., German D.A., Giaretta A., Gibernau M., Gillespie L.J., González C.C., Goyder D.J., Graham S.W., Grall A., Green L., Gunn B.F., Gutiérrez D.G., Hackel J., Haevermans T., Haigh A., Hall J.C., Hall T., Harrison M.J., Hatt S.A., Hidalgo O., Hodkinson T.R., Holmes G.D., Hopkins H.C.F., Jackson C.J., James S.A., Jobson R.W., Kadereit G., Kahandawala I.M., Kainulainen K., Kato M., Kellogg E.A., King G.J., Klejevskaja B., Klitgaard B.B., Klopper R.R., Knapp S., Koch M.A., Leebens-Mack J.H., Lens F., Leon C.J., Léveillé-Bourret É., Lewis G.P., Li D.Z., Li L., Liede-Schumann S., Livshultz T., Lorence D., Lu M., Lu-Irving P., Luber J., Lucas E.J., Luján M., Lum M., Macfarlane T.D., Magdalena C., Mansano V.F., Masters L.E., Mayo S.J., McColl K., McDonnell A.J., McDougall A.E., McLay T.G.B., McPherson H., Meneses R.I., Merckx V., Michelangeli F.A., Mitchell J.D., Monro A.K., Moore M.J., Mueller T.L., Mummenhoff K., Munzinger J., Muriel P., Murphy D.J., Nargar K., Nauheimer L., Nge F.J., Nyffeler R., Orejuela A., Ortiz E.M., Palazzesi L., Peixoto A.L., Pell S.K., Pellicer J., Penneys D.S., Perez-Escobar O.A., Persson C., Pignal M., Pillon Y., Pirani J.R., Plunkett G.M., Powell R.F., Prance G.T., Puglisi C., Qin M., Rabeler R.K., Rees P.E.J., Renner M., Roalson E.H., Rodda M., Rogers Z.S., Rokni S., Rutishauser R., de Salas M.F., Schaefer H., Schley R.J., Schmidt-Lebuhn A., Shapcott A., Al-Shehbaz I., Shepherd K.A., Simmons M.P., Simões A.O., Simões A.R.G., Siros M., Smidt E.C., Smith J.F., Snow N., Soltis D.E., Soltis P.S., Soreng R.J., Sothers C.A., Starr J.R., Stevens P.F., Straub S.C.K., Struwe L., Taylor J.M., Telford I.R.H., Thornhill A.H., Tooth I., Trias-Blasi A., Udovicic F., Utteridge T.M.A., Del Valle J.C., Verboom G.A., Vonow H.P., Vorontsova M.S., de Vos J.M., Al-Wattar N., Waycott M., Welker C.A.D., White A.J., Wieringa J.J., Williamson L.T., Wilson T.C., Wong S.Y., Woods L.A., Woods R., Worboys S., Xanthos M., Yang Y., Zhang Y.X., Zhou M.Y., Zmarzty S., Zuloaga F.O., Antonelli A., Bellot S., Crayn D.M., Grace O.M., Kersey P.J., Leitch I.J., Sauquet H., Smith S.A., Eiserhardt W.L., Forest F., Baker W.J. 2024. Phylogenomics and the rise of the angiosperms. Nature 629(8013):843–850.
Zuntini A.R., Frankel L.P., Pokorny L., Forest F., Baker W.J. 2021. A comprehensive phylogenomic study of the monocot order Commelinales, with a new classification of Commelinaceae. Am. J. Bot. 108(7):1066–1086.
Züst T., Strickler S.R., Powell A.F., Mabry M.E., An H., Mirzaei M., York T., Holland C.K., Kumar P., Erb M., Petschenka G., Gómez J.M., Perfectti F., Müller C., Pires J.C., Mueller L.A., Jander G. 2020. Independent evolution of ancestral and novel defenses in a genus of toxic plants (Erysimum, Brassicaceae). eLife. 9: 1–42.

https://doi.org/10.1093/sysbio/syag035
Advance Access publication April 20, 2026